STATISTICS, OPTIMIZATION AND INFORMATION COMPUTING
Stat., Optim. Inf. Comput., Vol. **10**, June 2022, pp 725–749.
Published online in International Academic Press (www.IAPress.org)

A Novel Two-parameter Nadarajah-Haghighi Extension: Properties, Copulas, Modeling Real Data and Different Estimation Methods

Wahid A. M. Shehata [1] and Haitham M. Yousof [2,*]

[1] *Department of Mathematics, Statistics and Insurance, Faculty of Business, Ain Shams University, Egypt*
[2] *Department of Statistics, Mathematics and Insurance, Benha University, Benha 13518, Egypt*

Abstract A new two-parameter lifetime distribution is proposed and numerically studied. The new model has a flexible failure rate shapes such as “monotonically increasing” , “monotonically decreasing” , “bathtub” , “constant” , “upside down” and “J-shape” . Various of its statistical properties are derived. A numerical analysis of skewness and kurtosis are presented. Many bivariate and multivariate extensions are also presented via Farlie Gumbel Morgenstern copula, Renyi entropy copula, modified Farlie Gumbel Morgenstern copula and Clayton copula. Several estimation methods such as the maximum likelihood, Cramer-von-Mises, L-moment estimation, Anderson Darling, right Tail-Anderson Darling estimation and left tail-Anderson Darling are presented and considered. Numerical simulations are performed to assess the performance of estimation methods. An environmental data set is employed to measure flexibility of the new model also to compare the estimation methods.

Keywords Lindley Family; Copulas; Anderson Darling estimation; Nadarajah Haghighi Model; Modeling; Cramér-vonMises; Entropy Index; L-moment estimation.

Mathematics Subject Classification: 60E05; 62N01; 62G05; 62N02; 62N05; 62E10; 62P30

DOI: 10.19139/soic-2310-5070-1250

1. Introduction and motivation

Lemonte [20] proposed a new three-parameter distribution with cumulative distribution function (CDF) presented as

$$\mathbf{G}_{\gamma,\tau,\lambda}(z) = \{1 - \exp[1 - (1 + z\lambda)^{\tau}]\}^{\gamma} \mid_{(z>0,\gamma>0,\tau>0 \text{ and } \lambda>0)},$$

which called the exponentiated Nadarajah-Haghighi (ENH). By considering the scale parameter $\lambda = 1$, the above CDF reduces to two-parameter ENH

$$G_{\gamma,\tau}(z) = [1 - \varsigma_{\tau,Z}(z)]^{\gamma} \mid_{(z>0,\gamma>0,\tau>0 \text{ and } \lambda>0)}, \tag{1}$$

where $\varsigma_{\tau,Z}(z) = \exp[1 - (1 + z)^{\tau}]$ and the corresponding probability density function (PDF) is

$$\mathbf{g}_{\gamma,\tau}(z) = \gamma\,\tau \frac{\varsigma_{\tau,Z}(z)\,(1 + z)^{\tau-1}}{[1 - \varsigma_{\tau,Z}(z)]^{1-\gamma}} \mid_{(z>0,\gamma>0 \text{ and } \tau>0)}. \tag{2}$$

The parameter γ and τ control the shape of the ENH distribution. For $\gamma = 1$, the ENH model reduces to the NH model (Nadarajah and Haghighi [30]). For $\tau = 1$, the ENH model reduces to the generalized exponential (GE)

---

*Correspondence to: Haitham M. Yousof (Email:haitham.yousof@fcom.bu.edu.eg). Department of Statistics, Mathematics and Insurance, Benha University, Benha 13518, Egypt

ISSN 2310-5070 (online) ISSN 2311-004X (print)

model (Gupta and Kundu [16]). For $\gamma = \tau = 1$, the ENH model reduces to the standard exponential (Exp) model. Recently, Yousof and Korkmaz [33] presented and studied the Topp-Leone Nadarajah-Haghighi distribution, Alizadeh et al. [5] presented the extended exponentiated Nadarajah-Haghighi model, Nascimento et al. [31] presented a new family called the odd Nadarajah-Haghighi family based on (1), Ibrahim [19] studied the odd log-logistic NH (OLLNH) model and finally Yousof et al. [38] proposed and studied a new lifetime model called the Topp Leone Generated Nadarajah Haghighi model. In this paper, we shall refer to the new distribution using (1) and (2) as the Lindley exponentiated Nadarajah Haghighi (LENH) model using the Lindley G (L-G) family of distributions which introduced by Silva et al. [37]. The PDF of the OL-G family of distributions are given by

$$f_{\underline{\Upsilon}}\left(z\right)=\frac{g_{\underline{\Upsilon}}\left(z\right)}{2\overline{G}_{\underline{\Upsilon}}\left(z\right)^{3}}\exp\left[-\mathbf{O}_{\underline{\Upsilon}}\left(z\right)\right]\mid_{(z\in\mathbf{R}^{+})}, \tag{3}$$

where $\mathbf{O}_{\underline{\Upsilon}}\left(z\right)=\frac{G_{\underline{\Upsilon}}(z)}{\overline{G}_{\underline{\Upsilon}}(z)}\mid_{(z\in\mathbf{R}^{+})}$ refers to the odd ratio, $G_{\underline{\Upsilon}}\left(z\right)$ is the CDF of the baseline model and $\overline{G}_{\underline{\Upsilon}}\left(z\right)=1-G_{\underline{\Upsilon}}\left(z\right)$ is the survival function of the baseline model and the corresponding PDF of (3) can be expressed as

$$F_{\underline{\Upsilon}}\left(z\right)=1-\frac{1+\overline{G}_{\underline{\Upsilon}}\left(z\right)}{2\overline{G}_{\underline{\Upsilon}}\left(z\right)}\exp\left[-\mathbf{O}_{\underline{\Upsilon}}\left(z\right)\right]\mid_{(z\in\mathbf{R}^{+})}, \tag{4}$$

respectively. In this paper, a new two-parameter lifetime distribution called the LENH model is proposed and studied. The new LENH model has a flexible hazard rate function (HRF). The HRF of the LENH model can be "monotonically increasing", "monotonically decreasing", "bathtub" and "upside down (reversed **U**)" (see Figure 2). The variance ($\mathbf{V}(Z)$), skewness ($\mathbf{S}(Z)$) and kurtosis ($\mathbf{K}(Z)$) measures of the LENH model can be calculated from its ordinary moments and the well-known relationships. Explicit mathematical expressions are derived for all its properties. Many bivariate LENH extensions are also presented. Several estimation methods such as the maximum likelihood estimation method, Cramér-von-Mises estimation method, L-moment estimation method, Anderson Darling estimation method, right tail-Anderson Darling estimation method, left tail-Anderson Darling estimation method are presented and considered. Numerical simulations are performed to assess the performance of estimation methods. Illustration of an environmental data set is employed to measure flexibility of the new model also to compare the estimation methods. Using (1), (2) and (3), we obtain the two-parameter LENH PDF as follows

$$f_{\underline{\Upsilon}}(z)=\frac{1}{2}\gamma\,\tau\left(1+z\right)^{\tau-1}\frac{\varsigma_{\tau,Z}\left(z\right)\left[1-\varsigma_{\tau,Z}\left(z\right)\right]^{\gamma-1}}{\left\{1-\left[1-\varsigma_{\tau,Z}\left(z\right)\right]^{\gamma}\right\}^{3}}\exp\left[-\frac{\left[1-\varsigma_{\tau,Z}\left(z\right)\right]^{\gamma}}{1-\left[1-\varsigma_{\tau,Z}\left(z\right)\right]^{\gamma}}\right], \tag{5}$$

where $z>0, \gamma>0$ and $\tau>0$. For $\gamma=1$, the LENH reduces to the Lindley NH (LNH) (Yousof et al. [42]). For $\gamma = \tau = 1$, the LENH model reduces to the Lindley generalized exponential (LGE) model. For $\gamma = \tau = 1$, the LENH model reduces to the Lindley exponential (LE) model. The proposed LENH distribution in (5) has a major advantage of having only two parameters γ and τ, consequently it provides an easier path in estimating its parameters, however many competitive models have three (or more) parameters as shown in Table 8. The corresponding CDF is given by

$$F_{\underline{\Upsilon}}(z)=1-\frac{1+\left(1-\left[1-\varsigma_{\tau,Z}\left(z\right)\right]^{\gamma}\right)}{2\left\{1-\left[1-\varsigma_{\tau,Z}\left(z\right)\right]^{\gamma}\right\}}\exp\left\{-\frac{\left[1-\varsigma_{\tau,Z}\left(z\right)\right]^{\gamma}}{1-\left[1-\varsigma_{\tau,Z}\left(z\right)\right]^{\gamma}}\right\}\mid_{(z>0,\gamma>0\text{ and }\tau>0)}. \tag{6}$$

The LENH density function can be expressed as an infinite mixture of ENH PDF as follows

$$f_{\underline{\Upsilon}}(z)=\sum_{\hbar_1,\hbar_2=0}^{\infty}\xi_{\hbar_1,\hbar_2}\mathbf{g}_{\gamma^*,\tau}\left(z\right)\mid_{\gamma^*=\gamma(\hbar_1+\hbar_2+1)}, \tag{7}$$

where

$$\xi_{\hbar_1,\hbar_2}=\frac{\left(-1\right)^{\hbar_2}\Gamma\left(\hbar_1+\hbar_2+3\right)}{2\left(\hbar_1+\hbar_2+1\right)\hbar_1!\hbar_2!\Gamma\left(\hbar_2+3\right)}.$$

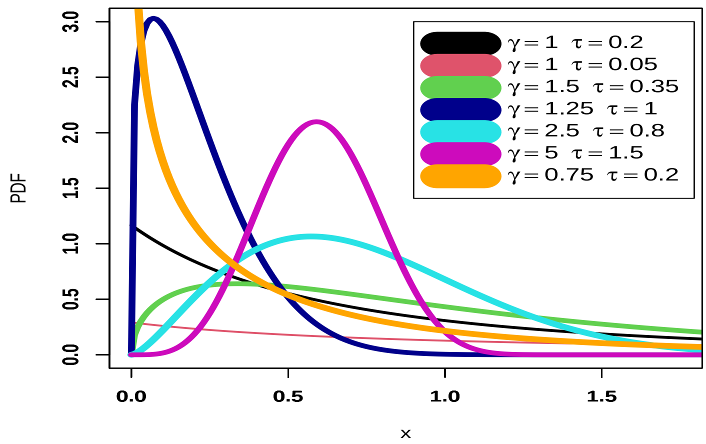

Figure 1. Plots of the LENH PDF for some parameter values.

and

$$\mathbf{g}_{\gamma^*,\tau}(z) = \gamma^* \tau \varsigma_{\tau,Z}(z)(1+z)^{\tau-1}\left[1-\varsigma_{\tau,Z}(z)\right]^{\gamma^*-1},$$

represents the ENH PDF with power parameter $\gamma^* > 0$. The CDF of LENH model can be given by integrating (7) as

$$F_{\underline{\Upsilon}}(z) = \sum_{\hbar_1,\hbar_2=0}^{\infty} \xi_{\hbar_1,\hbar_2}\mathbf{G}_{\gamma^*,\tau}(z), \tag{8}$$

where $\mathbf{G}_{\gamma^*,\tau}(z) = \left[1-\varsigma_{\tau,Z}(z)\right]^{\gamma^*}$ is the CDF of the ENH model with power parameter $\gamma^* > 0$. Figure 1 shows some plots of the LENH PDF for some parameter values. Figure 2 shows some plots of the LENH HRF for some parameter values.

We are motivated to present the LENH model for the following reasons:

- The LENH model has only two parameters among many other competitive model which have more than two parameters with less flexibility.
- The PDF of the LENH distribution can be "right skewed with heavy tail and one peak", "right skewed with heavy tail and no peak", "symmetric" and "semi-symmetric" (see Figure 1). Hence, the new model could be useful in modeling the right skewed real data with heavy tail and one peak, right skewed real data with heavy tail and no peak, symmetric and semi-symmetric real data sets.
- The new HRF accommodates "monotonically increasing", "monotonically decreasing", "**J**-HRF", "bathtub", "upside down" and "constant" (see Figure 2).
- The novel density can be simplified and re-expressed as a mixture representation of the ENH model which means that the properties of the novel density can be derived from the corresponding properties of the ENH model (see equation 7).
- The skewness ($\mathbf{S}(Z)$) of the LENH can range in the interval (0.4455, 33.07), whereas the $\mathbf{S}(Z)$ of the ENH varies only in the interval (0.51335, 3.5726). The kurtosis ($\mathbf{K}(Z)$) of the LENH is ranging from 2.8786 to 3749, whereas the $\mathbf{K}(Z)$ for the ENH only varies from 3.419 to 32.041. So it is clear that the new model is more flexible than the base line model (see Tables 1 and 2).
- The entropy index under the Rényi entropy confirm the wide flexibility of the LENH model.
- The new model proven its superiority in modeling the bimodal right skewed real data set (see subsection 6.2).

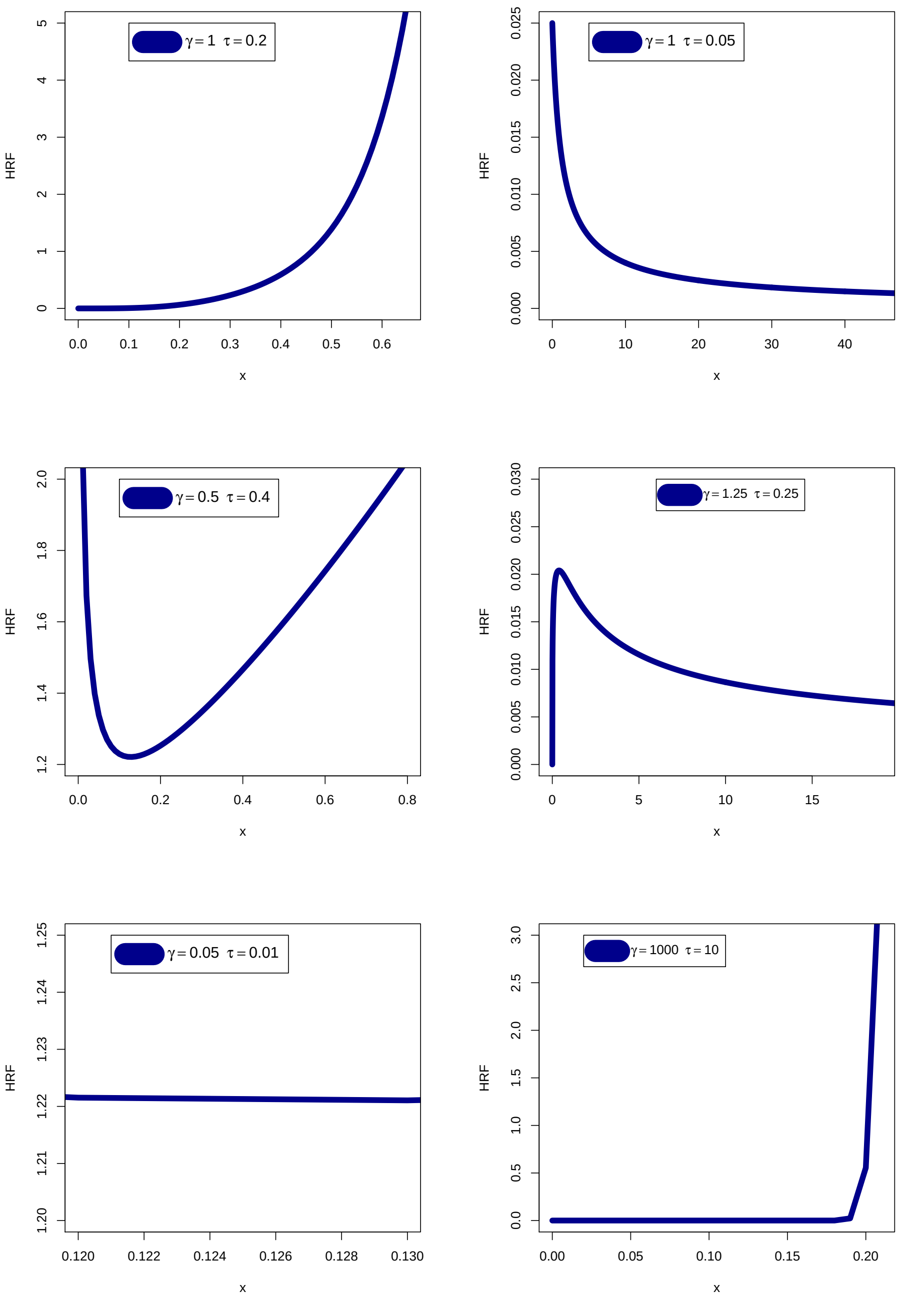

Figure 2. Plots of the LENH HRF for some parameter values.

Figure 1 shows that the LENH distribution has various PDF shapes such as "right skewed with heavy tail and one peak", "right skewed with heavy tail and no peak", "symmetric" and "semi-symmetric" densities. Figure 2 shows that the LENH model produces flexible hazard rate shapes such as "monotonically increasing"($\gamma = 1, \tau = 0.2$), "monotonically decreasing ($\gamma = 1, \tau = 0.05$)", "**J**-HRF ($\gamma = 1000, \tau = 10$)", "bathtub (or reversed upside down)

($\gamma = 0.5, \tau = 0.4$)", "upside down (reversed bathtub) ($\gamma = 1.65, \tau = 0.25$)" and "constant ($\gamma = 0.5, \tau = 0.4$)". These plots indicate that the LENH model is very useful in fitting different data sets with various shapes.

2. Properties

2.1. Moments and generating function

Table 1: $E(Z)$, $\mathbf{V}(Z)$, $\mathbf{S}(Z)$ and $\mathbf{K}(Z)$ of the LENH distribution.

γ	τ	$E(Z)$	$\mathbf{V}(Z)$	$\mathbf{S}(Z)$	$\mathbf{K}(Z)$
1.25	0.15	242.2539	188510.9	4.322433	33.86712
	0.20	50.09063	4324.717	2.758123	14.48364
	0.25	20.01207	458.0912	2.016948	8.687948
	0.35	20.01207	458.0912	2.016948	8.687948
3	0.2	207.5201	48891.94	2.046808	8.951579
	0.25	65.26315	3202.609	1.4921140	5.842854
	0.30	30.41397	510.8262	1.1459840	4.435005
	0.35	17.61411	134.7768	0.905572	3.686336
0.035	0.25	0.0021574	0.0001847	17.11736	529.9131
0.05		0.0102973	0.0019566	10.64658	199.1414
0.1		0.1107511	0.0788771	5.792837	59.0411
0.5		4.407403	35.82801	2.816552	14.97952
1		14.39430	255.1699	2.235054	10.03103
2		38.84068	1372.081	1.7112010	6.913076
5		117.9359	8316.892	1.2643050	4.901819
20		443.3004	67313.37	0.8387366	3.593372
50		896.2675	200394.2	0.6576252	3.207016
150		1834.271	601698.1	0.5021189	2.953407
250		2465.136	945190.5	**0.4454982**	**2.878647**
0.10	0.10	0.4873103	5.6566140	**33.07044**	**3749.32**
0.10	0.20	0.1494102	0.1661664	7.055457	94.48604
0.20	0.10	7.512419	1524.4640	28.89366	2294.686
0.25	0.15	3.728038	94.410400	8.414384	142.7792
0.15	0.25	0.3346136	0.4716986	4.603960	37.79379
0.10	0.50	0.04829055	0.0118380	4.247585	28.83613
0.55	0.15	32.63375	5228.0410	6.105494	69.34496

The rth moment of Z, say $\mu'_{\mathbf{r},Z}$, follows from (7) as

$$\mu'_{\mathbf{r},Z} = \mathbf{E}\left(Z^{\mathbf{r}}\right) = \sum_{\hbar_1,\hbar_2,\hbar_3=0}^{\infty} \sum_{\hbar_4=0}^{\mathbf{r}} \xi_{\hbar_1,\hbar_2}\, \eta_{\hbar_3,\hbar_4}^{(\gamma^*,\mathbf{r})} \Gamma\left(\frac{\hbar_4}{\tau}+1, 1+\hbar_3\right), \tag{9}$$

where

$$\eta_{\hbar_3,\hbar_4}^{(\gamma^*,\mathbf{r})} = \gamma^* \left(-1\right)^{\mathbf{r}+\hbar_3-\hbar_4} \left(1+\hbar_3\right)^{-\left(\frac{\hbar_4}{\tau}+1\right)} \exp\left(1+\hbar_3\right) \binom{\gamma^*-1}{\hbar_3} \binom{\mathbf{r}}{\hbar_4}.$$

Or

$$\mu'_{\mathbf{r},Z} = \mathbf{E}\left(Z^{\mathbf{r}}\right) = \sum_{\hbar_1,\hbar_2=0}^{\infty} \sum_{\hbar_3=0}^{\gamma^*-1} \sum_{\hbar_4=0}^{\mathbf{r}} \xi_{\hbar_1,\hbar_2}\, \eta_{\hbar_3,\hbar_4}^{(\gamma^*,\mathbf{r})} \Gamma\left(\frac{\hbar_4}{\tau}+1, 1+\hbar_3\right)|_{(\gamma^*>0 \text{ and integer})}.$$

The $\mathbf{V}(Z)$, $\mathbf{S}(Z)$ and $\mathbf{K}(Z)$ measures can be calculated from the ordinary moments in (9) and using well-known relationships. Table 1 give a numerical analysis for the $E(Z)$, $\mathbf{V}(Z)$, $\mathbf{S}(Z)$ and $\mathbf{K}(Z)$ for the LENH distribution. Based on Table 2 we note that:

- $\mathbf{S}(Z)$ of the LENH distribution always positive.
- $\mathbf{K}(Z)$ of the LENH distribution can be more than three or less than three.
- $E(Z)$ of the LENH model increases as γ increases.
- $E(Z)$ of the LENH model decreases as τ increases.
  Based on Tables 1 and 2 we note we can say that, the $\mathbf{S}(Z)$ of the LENH can range in the interval (**0.4455**, **33.07**), whereas the $\mathbf{S}(Z)$ of the ENH varies only in the interval (**0.51335**, **3.5726**). The spread for the LENH $\mathbf{K}(Z)$ is ranging from **2.8786** to **3749**, whereas the spread for the ENH $\mathbf{K}(Z)$ only varies from **3.419** to **32.041**. So it is clear that the new model is more flexible than the base line model.

Table 2: $E(z)$, $\mathbf{V}(z)$, $\mathbf{S}(z)$ and $\mathbf{K}(z)$ of the ENH distribution.

γ	τ	$E(z)$	$\mathbf{V}(z)$	$\mathbf{S}(z)$	$\mathbf{K}(z)$
1	1	1	1	2	9
2		1.5	1.25	1.609969	7.08
5		2.283333	1.463611	1.339221	6.025973
10		2.928968	1.549768	1.241416	5.703086
20		3.597740	1.596163	1.190993	5.548813
50		4.499205	1.625133	1.160248	5.458834
75		4.901356	1.631689	1.153366	5.439116
100		5.187378	1.634984	1.149918	5.429296
200		5.878031	1.639947	1.144738	5.414611
500		6.792823	1.642936	1.141626	5.405815
100	0.35	203.6261	21037.49	**3.572594**	**32.04097**
	0.40	102.1248	3740.145	2.886795	20.84275
	0.45	59.77733	964.0727	2.453066	15.39329
	0.50	38.91862	321.711	2.153882	12.30458
	0.75	10.46292	10.47627	1.437076	6.893606
	1.00	5.187378	1.634984	1.149918	5.429296
	2.00	1.475057	0.0614697	0.7767964	4.056221
	3	0.8277548	0.0146344	0.6639387	3.750942
	5	0.4352452	0.0032054	0.5769205	3.548918
	10	0.1977865	0.0005529	**0.5133473**	**3.419141**
10	10	0.1419304	0.0011704	0.3408162	3.095872
0.1	10	0.01060546	0.0006629	3.506997	17.17571
1	30	0.02017738	0.0002059	0.2755712	3.52802
30	1	3.994987	1.612150	1.173958	5.498575

Bowley's $\mathbf{S}(z)$ and the Moors' $\mathbf{K}(z)$ can be calculated and then sketched using the quantile function (QF) ($\mathbf{Q}^{(\cdot)}$). The Bowley's $\mathbf{S}(z)$ is based on quartiles given by

$$\mathbf{S}\left(z\right)=\frac{\mathbf{Q}^{\left(\frac{3}{4}\right)}-2\mathbf{Q}^{\left(\frac{2}{4}\right)}+\mathbf{Q}^{\left(\frac{1}{4}\right)}}{\mathbf{Q}^{\left(\frac{3}{4}\right)}-\mathbf{Q}^{\left(\frac{1}{4}\right)}},$$

and the Moor's $\mathbf{K}(z)$, see Moors (1998), is given by

$$\mathbf{K}\left(z\right)=\frac{\mathbf{Q}^{\left(\frac{7}{8}\right)}-\mathbf{Q}^{\left(\frac{5}{8}\right)}+\mathbf{Q}^{\left(\frac{3}{8}\right)}-\mathbf{Q}^{\left(\frac{1}{8}\right)}}{\mathbf{Q}^{\left(\frac{6}{8}\right)}-\mathbf{Q}^{\left(\frac{2}{8}\right)}},$$

where $\mathbf{Q}(.)$ is the QF. Figure 3 indicates that $\mathbf{S}(z)$ and depend very much on the shape parameters γ and τ. Here, we provide two formulae for the MGF $M_Z\left(t\right)=\mathbf{E}\left(\exp\left(\mathrm{e}^{t\,Z}\right)\right)$ of z. Clearly, the first one can be derived using (7) as

$$M_Z\left(t\right)=\sum_{\hbar_1,\hbar_2,\hbar_3,\mathbf{r}=0}^{\infty}\sum_{\hbar_4=0}^{\mathbf{r}}\xi_{\hbar_1,\hbar_2}\frac{t^{\mathbf{r}}}{\mathbf{r}!}\eta_{\hbar_3,\hbar_4}^{(\gamma^*,\mathbf{r})}\Gamma\left(\frac{\hbar_4}{\tau}+1,1+\hbar_3\right).$$

Or

$$M_Z\left(t\right)=\sum_{\hbar_1,\hbar_2,\mathbf{r}=0}^{\infty}\sum_{\hbar_3=0}^{\gamma^*-1}\sum_{\hbar_4=0}^{\mathbf{r}}\xi_{\hbar_1,\hbar_2}\frac{t^{\mathbf{r}}}{\mathbf{r}!}\eta_{\hbar_3,\hbar_4}^{(\gamma^*,\mathbf{r})}\Gamma\left(\frac{\hbar_4}{\tau}+1,1+\hbar_3\right)|_{(\gamma^*>0\text{ and integer})}.$$

2.2. Incomplete moments

The rth incomplete moment, say $\mathbf{I}_{\mathbf{r},Z}\left(Z\right)$, of Z can be expressed using (7) as

$$\mathbf{I}_{\mathbf{r},Z}\left(Z\right)=\sum_{\hbar_1,\hbar_2,\hbar_3=0}^{\infty}\sum_{\hbar_4=0}^{\mathbf{r}}\xi_{\hbar_1,\hbar_2}\eta_{\hbar_3,\hbar_4}^{(\gamma^*,\mathbf{r})}\left[\begin{array}{c}\Gamma\left(\frac{\hbar_4}{\tau}+1,1+\hbar_3\right)\\-\Gamma\left(\frac{\hbar_4}{\tau}+1,\left(1+\hbar_3\right)\left(1+b\,z\right)^{\tau}\right)\end{array}\right]. \tag{10}$$

Or

$$\mathbf{I}_{\mathbf{r},Z}\left(Z\right)=\sum_{\hbar_1,\hbar_2=0}^{\infty}\sum_{\hbar_3=0}^{\gamma^*-1}\sum_{\hbar_4=0}^{\mathbf{r}}\xi_{\hbar_1,\hbar_2}\eta_{\hbar_3,\hbar_4}^{(\gamma^*,\mathbf{r})}\left[\begin{array}{c}\Gamma\left(\frac{\hbar_4}{\tau}+1,1+\hbar_3\right)\\-\Gamma\left(\frac{\hbar_4}{\tau}+1,\left(1+\hbar_3\right)\left(1+b\,z\right)^{\tau}\right)\end{array}\right]|_{(\gamma^*>0\text{ and integer})}.$$

The mean deviations about the mean $[\delta_{1,Z}=\mathbf{E}(|z-\mu'_{1,Z}|)]$ and about the median $\left[\delta_{2,Z}=\mathbf{E}\left(|Z-M|\right)\right]$ of z are given by $\delta_{1,Z}=2\mu'_{1,Z}F(\mu'_{1,Z})-2\mathbf{I}_{1,Z}(\mu'_{1,Z})$ and $\delta_{2,Z}=\mu'_{1,Z}-2\mathbf{I}_{1,Z}\left(M\right)$, respectively, where $\mu'_{1,Z}=\mathbf{E}\left(Z\right)$, $M=$Median$(Z)=Q\left(\frac{1}{2}\right)$ is the median, $F(\mu'_{1,Z})$ is easily calculated from (6) and $\mathbf{I}_{1,Z}\left(z\right)$ is the first incomplete moment given by (10) with $r=1$.

2.3. Moment of residual life and reversed residual life

The rth moment of the residual life $l_{\mathbf{r},Z}(t)=\mathbf{E}[(Z-t)^{\mathbf{r}}]\mid_{(Z>t\text{ and }\mathbf{r}=1,2,\ldots)}$. The rth moment of the residual life of Z is given by

$$l_{\mathbf{r},Z}(t)=\frac{1}{1-F_{\underline{\Upsilon}}(t)}\int_z^{\infty}(Z-t)^{\mathbf{r}}dF_{\underline{\Upsilon}}(z).$$

Therefore

$$l_{\mathbf{r},Z}(t)=\frac{1}{1-F_{\underline{\Upsilon}}(z)}\sum_{\hbar_1,\hbar_2,\hbar_3=0}^{\infty}\sum_{\hbar_4=0}^{\mathbf{r}}\xi_{\hbar_1,\hbar_2}^{(1)}\eta_{\hbar_3,\hbar_4}^{(\gamma^*,\mathbf{r})}\Gamma\left(\frac{\hbar_4}{\tau}+1,1+\hbar_3\right),$$

where

$$\xi_{\hbar_1,\hbar_2}^{(1)}=\xi_{\hbar_1,\hbar_2}\sum_{h=0}^{n}(-1)^{n-h}\binom{n}{h}z^{n-h}.$$

Or

$$l_{\mathbf{r},Z}(t)=\frac{1}{1-F_{\underline{\Upsilon}}(t)}\sum_{\hbar_1,\hbar_2=0}^{\infty}\sum_{\hbar_3=0}^{\gamma^*-1}\sum_{\hbar_4=0}^{\mathbf{r}}\xi^{(1)}_{\hbar_1,\hbar_2}\eta^{(\gamma^*,\mathbf{r})}_{\hbar_3,\hbar_4}\Gamma\left(\frac{\hbar_4}{\tau}+1,1+\hbar_3\right)|_{(\gamma^*>0\text{ and integer})}.$$

The rth moment of the reversed residual life

$$L_{\mathbf{r},Z}(t)=\mathbf{E}\left[(t-Z)^{\mathbf{r}}\right]|_{(Z\leq t,\, t>0\text{ and }\mathbf{r}=1,2,\dots)}.$$

Then. we have

$$L_{\mathbf{r},Z}(t)=\frac{1}{F_{\underline{\Upsilon}}(z)}\int_0^z (t-Z)^{\mathbf{r}}dF_{\underline{\Upsilon}}(z).$$

Then, the rth moment of the reversed residual life of Z becomes

$$L_{\mathbf{r},Z}(z)=\frac{1}{F_{\underline{\Upsilon}}(t)}\sum_{\hbar_1,\hbar_2,\hbar_3=0}^{\infty}\sum_{\hbar_4=0}^{\mathbf{r}}\xi^{(2)}_{\hbar_1,\hbar_2}\eta^{(\gamma^*,\mathbf{r})}_{\hbar_3,\hbar_4}\begin{bmatrix}\Gamma\left(\frac{\hbar_4}{\tau}+1,1+\hbar_3\right)\\ -\Gamma\left(\frac{\hbar_4}{\tau}+1,(1+\hbar_3)\left(1+b\,z\right)^{\tau}\right)\end{bmatrix},$$

where

$$\xi^{(2)}_{\hbar_1,\hbar_2}=\xi_{\hbar_1,\hbar_2}\sum_{h=0}^{n}(-1)^h\binom{n}{h}z^{n-h}.$$

Or

$$L_{\mathbf{r},Z}(t)=\frac{1}{F_{\underline{\Upsilon}}(z)}\sum_{\hbar_1,\hbar_2=0}^{\infty}\sum_{\hbar_3=0}^{\gamma^*-1}\sum_{\hbar_4=0}^{\mathbf{r}}\xi^{(2)}_{\hbar_1,\hbar_2}\eta^{(\gamma^*,\mathbf{r})}_{\hbar_3,\hbar_4}\begin{bmatrix}\Gamma\left(\frac{\hbar_4}{\tau}+1,1+\hbar_3\right)\\ -\Gamma\left(\frac{\hbar_4}{\tau}+1,(1+\hbar_3)\left(1+b\,z\right)^{\tau}\right)\end{bmatrix}|_{(\gamma^*>0\text{ and integer})}.$$

2.4. Order statistics

Suppose $Z_1, Z_2, \dots, Z_n$ is a random sample from an LENH model. Let $Z_{i:n}$ denote the ith order statistic. The PDF of $Z_{i:n}$ can be expressed as

$$f_{i:n}(z)=\frac{f_{\underline{\Upsilon}}(z)}{B(i,n-i+1)}F_{\underline{\Upsilon}}(z)^{i-1}\left[1-F_{\underline{\Upsilon}}(z)\right]^{n-i}. \tag{11}$$

We can write the density function of $Z_{i:n}$ in (11) as

$$f_{i:n}(z)=\sum_{\nu_1,p=0}^{\infty}\sum_{\nu_3=0}^{\nu_2+n-i}\upsilon_{\nu_1,\nu_3,p}\,\mathbf{g}_{\gamma^{\cdot},\tau}(z)|_{\gamma^{\cdot}=(i_3+i_1+p)\gamma}, \tag{12}$$

where

$$\upsilon_{\nu_1,\nu_3,p}=\sum_{\nu_2=0}^{n-1}\frac{(-1)^{\nu 2+\nu_1}}{B(i,n-i+1)\nu_1!\left[\gamma^{\cdot}+1\right]}\binom{\gamma^{\cdot}}{\nu_3+\nu_1}\binom{i_2+n-i}{\nu_3}\binom{i-1}{\nu_2}.$$

Equation (12) is the main result of this section. It reveals that the PDF of the LENH order statistics is a linear combination of ENH density functions. So, several mathematical quantities of the LENH order statistic such as ordinary, incomplete and factorial moments, mean deviations and several others can be determined from those quantities of the ENH distribution. The pth moment of $Z_{i:n}$ is given by

$$\mathbf{E}(Z^p_{i:n})=\sum_{\nu_1,p,w=0}^{\infty}\sum_{\nu_2=0}^{\nu_2+n-i}\sum_{l=0}^{\mathbf{r}}\upsilon_{\nu_1,\nu_3,p}\,\eta^{(\gamma^{\cdot},\mathbf{r})}_{i_3,i}\Gamma\left(\frac{l}{\tau}+1,1+w\right). \tag{13}$$

Or

$$\mathbf{E}(Z^p_{i:n})=\sum_{i_1,p=0}^{\infty}\sum_{\nu_3=0}^{\nu_2+n-i}\sum_{l=0}^{\mathbf{r}}\sum_{w=0}^{\gamma^{\cdot}-1}\upsilon_{\nu_1,\nu_3,p}\,\eta^{[\gamma^{\cdot},\mathbf{r}]}_{\nu_3,i}\Gamma\left(\frac{l}{\tau}+1,1+w\right)|_{(\gamma^{\cdot}>0\text{ and integer})}.$$

2.5. *Entropy index*

An entropy is a measure of variation or uncertainty of a random variable Z. Two popular entropy measures are due to Rényi [35] and Shannon [36]. The Rényi entropy of a random variable with PDF $f(z)$ is defined by

$$R_Z(\delta) = \frac{1}{1-\delta} \log \left(\int_0^\infty f^\delta(z) dz \right),$$

for $\delta > 0$ and $\delta \neq 1$. Then

$$R_Z(\delta) = \frac{\left(\frac{1}{2}\gamma\tau\right)^\delta}{1-\delta} \log \left(\int_0^\infty (1+z)^{\delta(\tau-1)} \frac{\varsigma_\tau^\delta(z) \left[1-\varsigma_{\tau,Z}(z)\right]^{\delta(\gamma-1)}}{\left\{1-\left[1-\varsigma_{\tau,Z}(z)\right]^\gamma\right\}^{3\delta}} \exp\left[-\delta \frac{\left[1-\varsigma_{\tau,Z}(z)\right]^\gamma}{1-\left[1-\varsigma_{\tau,Z}(z)\right]^\gamma}\right] dz \right).$$

Instead of the mathematical analyzing the above equation, we can graphically analyze it. Figure 3 gives graphical entropy index under the Rényi entropy. Based on Figure 3, the Rényi entropy of the new distribution can have some useful shapes. The plots of Figure 3 are sketched using different combinations of parameters.

3. Copula

Following Al-babtain et al. [4], Yousof et al. [41], Mansour et al. ([23],[24],[25],[26],[27],[27]), Elgohari and Yousof ([28], [14]), Ali et al. ([2],[3]), we derive some new bivariate type LENH (Biv-LENH) model using Farlie Gumbel Morgenstern (FGM) Copula(see Morgenstern [29], Gumbel [17] and Gumbel [18]), modified FGM Copula (see Rodriguez-Lallena and Ubeda-Flores [34]), Clayton Copula and Renyi's entropy (Pougaza and Djafari [33]). The Multivariate LENH (MvLENH) type is also presented. However, future works may be allocated to study these new models. First, we consider the joint CDF of the FGM family, where

$$\mathtt{C}_\nabla(\mu,\nu) = \mu\nu\left(1+\nabla\mu^*\nu^*\right)|_{\mu^*=1-\mu},$$

where the marginal function $\mu = F_1$, $\nu = F_2$, $\nabla \in (-1,1)$ is a dependence parameter and for every $\mu, \nu \in (0,1)$, $\mathtt{C}(\mu,0) = \mathtt{C}(0,\nu) = 0$ which is "grounded minimum" and $\mathtt{C}(\mu,1) = \mu$ and $\mathtt{C}(1,\nu) = \nu$ which is "grounded maximum", $\mathtt{C}(\mu_1,\nu_1) + \mathtt{C}(\mu_2,\nu_2) - \mathtt{C}(\mu_1,\nu_2) - \mathtt{C}(\mu_2,\nu_1) \geq 0$.

3.1. *Via FGM Copula*

A Copula is continuous in μ and ν; actually, it satisfies the stronger Lipschitz condition, where

$$|\mathtt{C}(\mu_2,\nu_2) - \mathtt{C}(\mu_1,\nu_1)| \leq |\mu_2-\mu_1| + |\nu_2-\nu_1|.$$

For $0 \leq \mu_1 \leq \mu_2 \leq 1$ and $0 \leq \nu_1 \leq \nu_2 \leq 1$, we have

$$\Pr(\mu_1 \leq \mu \leq \mu_2, \nu_1 \leq W \leq \nu_2) = \mathtt{C}(\mu_1,\nu_1) + \mathtt{C}(\mu_2,\nu_2) - \mathtt{C}(\mu_1,\nu_2) - \mathtt{C}(\mu_2,\nu_1) \geq 0.$$

Then, setting $\mu^* = 1 - F_{\underline{\Upsilon}_1}(x_1)|_{[\mu^*=(1-\mu)\in(0,1)]}$ and $\nu^* = 1 - F_{\underline{\Upsilon}_2}(x_2)|_{[\nu^*=(1-\nu)\in(0,1)]}$. We can esaily get the get the joint CDF of the FGM family. The joint PDF can then derived from $c_\nabla(\mu,\nu) = 1 + \nabla\mu^{\cdot}\nu^{\cdot}|_{(\mu^{\cdot}=1-2\mu \text{ and } \nu^{\cdot}=1-2\nu)}$ or from $f(x_1,x_2) = \mathtt{C}(F_1,F_2)f_1f_2$.

3.2. *Via modified FGM Copula*

The modified FGM copula is defined as

$$\mathtt{C}_\nabla(\mu,\nu) = \mu\nu\left[1+\nabla\psi(\mu)\vartheta(\nu)\right]|_{\nabla\in(-1,1)}$$

or

$$\mathtt{C}_\nabla(\mu,\nu) = \mu\nu + \nabla\widetilde{\psi}_\mu\widetilde{\vartheta}_\nu|_{\nabla\in(-1,1)},$$

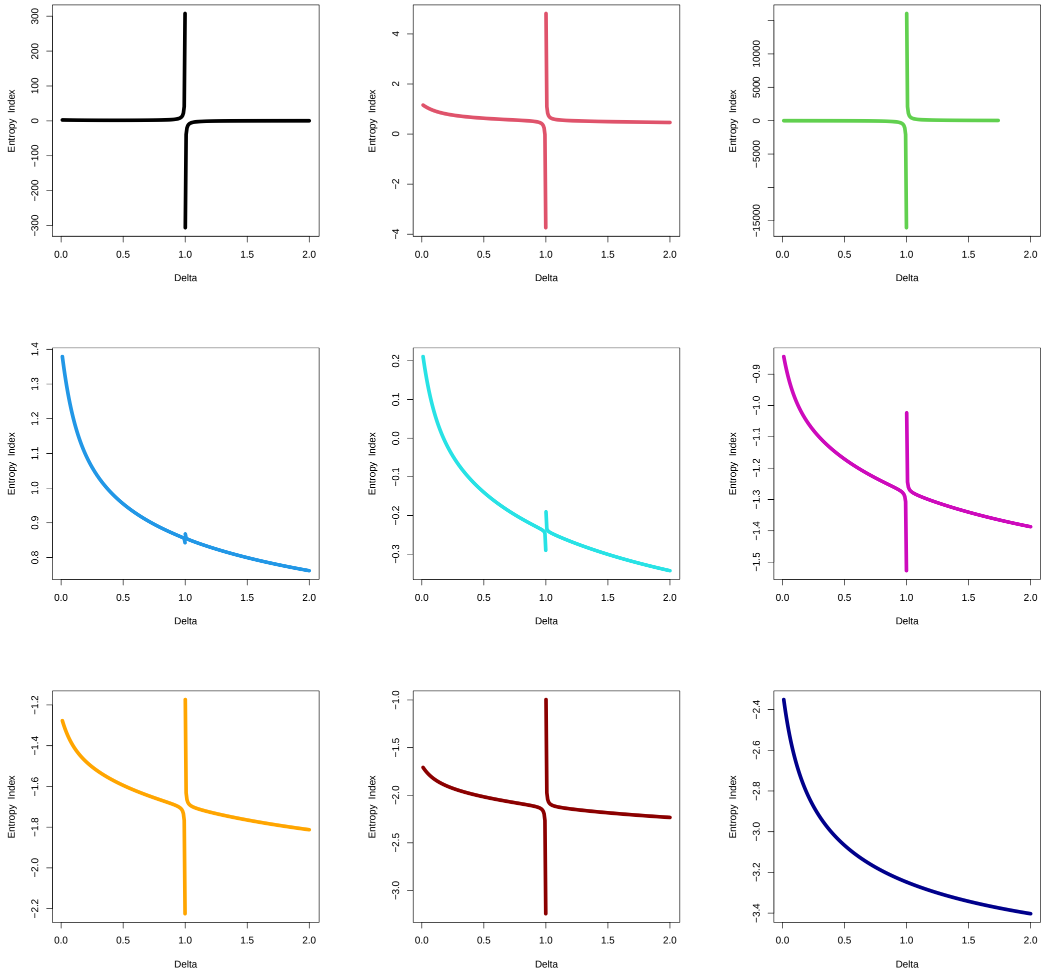

Figure 3. Graphical entropy index under Rényi entropy.

where $\widetilde{\psi}_\mu = \mu\psi(\mu)$, and $\widetilde{\vartheta}_\nu = \nu\vartheta(\nu)$. Where $\psi(\mu)$ and $\vartheta(\nu)$ are two continuous functions on $(0,1)$ where $\psi(0) = \psi(1) = \vartheta(0) = \vartheta(1) = 0$. Let

$$a_1 = \inf\left\{\widetilde{\psi}_\mu : \frac{\partial}{\partial\mu}\widetilde{\psi}_\mu|_{\sigma_1}\right\} < 0, a_2 = \sup\left\{\widetilde{\psi}_\mu : \frac{\partial}{\partial\mu}\widetilde{\psi}_\mu|_{\sigma_1}\right\} < 0,$$

$$b_1 = \inf\left\{\widetilde{\vartheta}_\nu : \frac{\partial}{\partial\nu}\widetilde{\vartheta}_\nu|_{\sigma_2}\right\} > 0, b_2 = \sup\left\{\widetilde{\vartheta}_\nu : \frac{\partial}{\partial\nu}\widetilde{\vartheta}_\nu|_{\sigma_2}\right\} > 0.$$

Then, $1 \leq \min(a_1a_2, b_1b_2) < \infty$, where

$$\mu\frac{\partial}{\partial\mu}\psi(\mu) = \frac{\partial}{\partial\mu}\widetilde{\psi}_\mu - \psi(\mu),$$

$$\sigma_1 = \left\{\mu : \mu \in (0,1)\,|_{\frac{\partial}{\partial\mu}\widetilde{\psi}_\mu \text{ exists}}\right\}$$

and

$$\sigma_2 = \left\{ \nu : \nu \in (0,1) \,|_{\frac{\partial}{\partial \nu} \widetilde{\vartheta}_\nu \text{ exists}} \right\}.$$

3.2.1. Biv-LENH-FGM (Type-I) model Consider the following functional form for both $\psi(\mu)$ and $\vartheta(\nu)$. Then, the Biv-LENH-FGM (Type-I) can be derived from $\mathsf{C}_\nabla(\mu,\nu) = \mu\nu + \nabla \widetilde{\psi}_\mu \widetilde{\vartheta}_\nu |_{\nabla \in (-1,1)}$ where $\widetilde{\psi}_\mu = \mu \left[1 - F_{\underline{\Upsilon}_1}(\mu)\right]$ and $\widetilde{\vartheta}_\nu = \nu \left[1 - F_{\underline{\Upsilon}_2}(\nu)\right]$.

3.2.2. Biv-LENH-FGM (Type-II) model Let $\psi(\mu)$ and $\vartheta(\nu)$ be two functional form for satisfy all the conditions stated earlier where

$$\psi(\mu)^* \,|_{(\nabla_1 > 0)} = \mu^{\nabla_1} (1-\mu)^{1-\nabla_1}$$

and

$$\vartheta(\nu)^* \,|_{(\nabla_2 > 0)} = \nu^{\nabla_2} (1-\nu)^{1-\nabla_2}.$$

Then, the corresponding Biv-LENH-FGM **(**Type-**II)** can be derived from

$$\mathsf{C}_{\nabla,\nabla_1,\nabla_2}(\mu,\nu) = \mu\nu \left[1 + \nabla \psi(\mu)^* \; \vartheta(\nu)^*\right].$$

3.2.3. Biv-LENH-FGM (Type-III) model Let $\widetilde{\psi^*(\mu)} = \mu\left[\log(1+\mu^*)\right]$ and $\widetilde{\vartheta^*(\nu)} = \nu\left[\log(1+\nu^*)\right]$ for all $\psi(\mu)$ and $\vartheta(\nu)$ which satisfies all the conditions stated earlier. In this case, one can also derive a closed form expression for the associated CDF of the Biv-LENH-FGM (Type-**III**) from

$$\mathsf{C}_\nabla(\mu,\nu) = \mu\nu \left(1 + \nabla \widetilde{\psi^*(\mu)}\, \widetilde{\vartheta^*(\nu)}\right).$$

3.3. Via Clayton Copula

The Clayton Copula can be considered as

$$\mathsf{C}(\nu_1,\nu_2) = \left[(1/\nu_1)^\nabla + (1/\nu_2)^\nabla - 1\right]^{-\nabla^{-1}} |_{\nabla \in (0,\infty)}.$$

Setting $\nu_1 = F_{\underline{\Upsilon}_1}(t)$ and $\nu_2 = F_{\underline{\Upsilon}_2}(x)$. Then, the Biv-LENH type can be derived from $\mathsf{C}(\nu_1,\nu_2) = \mathsf{C}(F_{\vartheta_1}(t), F_{\vartheta_2}(x))$. Similarly, the MvLENH **(**m-dimensional extension) from the above can be derived from

$$\mathsf{C}(\nu_\hbar) = \left(\sum_{\hbar=1}^{m} \nu_\hbar^{-\nabla} + 1 - m\right)^{-\nabla^{-1}}.$$

3.4. Via Renyi's entropy

Using the theorem of Pougaza and Djafari (2011) where

$$\mathsf{C}(\mu,\nu) = x_2\mu + x_1\nu - x_1x_2.$$

Then, the associated Biv-LENH will be $\mathsf{C}(u,\nu) = \mathsf{C}(F_{\underline{\Upsilon}_1}(x_1), F_{\underline{\Upsilon}_2}(x_2))$.

4. Estimation

In this Section we will consider the following estimation methods:

- Maximum likelihood estimation (MLE) method.
- Cramér-von-Mises estimation (CVME) method.

- L-moment estimation method.
- Anderson Darling estimation (ADE) method.
- Right Tail-Anderson Darling estimation (RADE) method.
- Lest Tail-Anderson Darling estimation (LADE) method.

4.1. MLE

Let $z_1, z_2, \ldots, z_n$ be a random sample from this distribution with parameter vector $\underline{\boldsymbol{\Upsilon}} = (\gamma,\tau)^\intercal$. The log-likelihood (Log-L) function for $\underline{\boldsymbol{\Upsilon}}$, say $\ell(\underline{\boldsymbol{\Upsilon}})$, is given by

$$\begin{aligned}\ell\left(\underline{\boldsymbol{\Upsilon}}\right) \quad = \quad & n\log\left(\frac{1}{2}\right)+n\log\left(\gamma\right)+n\log\left(\tau\right)+\sum_{\hbar=0}^{n}\left[1-\left(1+z_{\hbar,n}\right)^{\tau}\right] \\ & +\left(\tau-1\right)\sum_{\hbar=0}^{n}\log(1+z_{\hbar,n})+\left(\gamma-1\right)\sum_{\hbar=0}^{n}\log\left(1-\varsigma_{\tau,Z_{\hbar,n}}\left(z_{\hbar,n}\right)\right) \\ & -3\sum_{\hbar=0}^{n}\log\left[1-\left(1-a_{\hbar}\right)^{\gamma}\right]-\sum_{\hbar=0}^{n}\frac{\left[1-\varsigma_{\tau,Z_{\hbar,n}}\left(z_{\hbar,n}\right)\right]^{\gamma}}{1-\left[1-\varsigma_{\tau,Z_{\hbar,n}}\left(z_{\hbar,n}\right)\right]^{\gamma}}.14 \end{aligned} \tag{1}$$

The last equation can be maximized either by using the different programs like `R` (`optim` function), `SAS` (`PROC NLMIXED`) or by solving the nonlinear likelihood equations obtained by differentiating (14). The score vector elements, $\mu\underline{\boldsymbol{\Upsilon}} = \left(\frac{\partial\ell}{\partial\gamma}, \frac{\partial\ell}{\partial\tau}\right)^\intercal$, are easily to be derived.

4.2. CVME

MacDonald [22] proposed the CVME method based on the theory of minimum distance estimation. The CVMEof the parameter γ and τ are obtained by minimizing the following expression with respect to (wrt) to the parameters γ and τ respectively.

$$\mathbf{CVM}_{\underline{\boldsymbol{\Upsilon}}} = \frac{1}{12n} + \sum_{\hbar=1}^{n}\left[F_{(\gamma,\tau)}(z_{\hbar:n}) - c_{\hbar,n}\right]^2,$$

where $c_{\hbar,n} = \frac{2\hbar-1}{2n}$ and

$$\mathbf{CVM}_{(\underline{\boldsymbol{\Upsilon}})} = \frac{1}{12n} + \sum_{\hbar=1}^{n}\left(\left\{\begin{array}{c} 1-\frac{1+\left\{1-\left[1-\varsigma_{\tau,Z_{\hbar,n}}(z_{\hbar,n})\right]^{\gamma}\right\}}{2\left\{1-\left[1-\varsigma_{\tau,Z_{\hbar,n}}(z_{\hbar,n})\right]^{\gamma}\right\}} \\ \times\exp\left\{-\frac{\left[1-\varsigma_{\tau,Z_{\hbar,n}}(z_{\hbar,n})\right]^{\gamma}}{1-\left[1-\varsigma_{\tau,Z_{\hbar,n}}(z_{\hbar,n})\right]^{\gamma}}\right\}\end{array}\right\} - c_{\hbar,n}\right)^2.$$

Then, CVME of the parameters γ and τ are obtained by solving the two following non-linear equations

$$\sum_{\hbar=1}^{n}\left(\left\{\begin{array}{c} 1-\frac{1+\left\{1-\left[1-\varsigma_{\tau,Z_{\hbar,n}}(z_{\hbar,n})\right]^{\gamma}\right\}}{2\left\{1-\left[1-\varsigma_{\tau,Z_{\hbar,n}}(z_{\hbar,n})\right]^{\gamma}\right\}} \\ \times\exp\left\{-\frac{\left[1-\varsigma_{\tau,Z_{\hbar,n}}(z_{\hbar,n})\right]^{\gamma}}{1-\left[1-\varsigma_{\tau,Z_{\hbar,n}}(z_{\hbar,n})\right]^{\gamma}}\right\}\end{array}\right\} - c_{\hbar,n}\right)\eta_{(\gamma)}(z_{\hbar,n},\gamma,\tau) = 0,$$

and

$$\sum_{\hbar=1}^{n}\left(\left\{\begin{array}{c} 1-\frac{1+\left\{1-\left[1-\varsigma_{\tau,Z_{\hbar,n}}(z_{\hbar,n})\right]^{\gamma}\right\}}{2\left\{1-\left[1-\varsigma_{\tau,Z_{\hbar,n}}(z_{\hbar,n})\right]^{\gamma}\right\}} \\ \times\exp\left\{-\frac{\left[1-\varsigma_{\tau,Z_{\hbar,n}}(z_{\hbar,n})\right]^{\gamma}}{1-\left[1-\varsigma_{\tau,Z_{\hbar,n}}(z_{\hbar,n})\right]^{\gamma}}\right\}\end{array}\right\} - c_{\hbar,n}\right)\eta_{(\tau)}(z_{\hbar,n},\gamma,\tau) = 0,$$

where $\eta_{(\gamma)}(z_{\hbar,n},\gamma,\tau)$ and $\eta_{(\tau)}(z_{\hbar,n},\gamma,\tau)$ are the values of the first derivatives of the cdf of OLENG distribution wrt γ and τ respectively.

4.3. L-moment estimation

Based upon the moments of the order statistics, we can derive explicit expressions for the L-moments of Z as infinite weighted linear combinations of the means of suitable OLENG order statistics. The L-moments for the population can be obtained from

$$_{\mathbf{r}} = \frac{1}{\mathbf{r}} \sum_{m=0}^{\mathbf{r}-1} (-1)^m \binom{\mathbf{r}-1}{m} \mathbf{E}(Z_{\mathbf{r}-m:m})|_{\ (\mathbf{r}\geq 1)}.$$

The first four L-moments are given by

$$_{1}(\gamma, \tau) = \mathbf{E}(Z_{1:1}) = \mu_1' = \ell_1,$$

$$_{2}(\gamma, \tau) = \frac{1}{2}\mathbf{E}(Z_{2:2} - Z_{1:2}) = \frac{1}{2}(\mu_{2:2}' - \mu_{1:2}') = \ell_2,$$

where $\ell_{\hbar}|_{(\hbar=1.2)}$ is the L-moments for the sample. Then The L-moments estimators $\widehat{\gamma}_{\text{(L-moment)}}$ and $\widehat{\tau}_{\text{(L-moment)}}$ of the parameters γ and τ can be obtained by solving the following four equations numerically

$$_{1}\left(\widehat{\gamma}_{\text{(L-moment)}} \text{ and } \widehat{\tau}_{\text{(L-moment)}}\right) = \ell_1,$$

and

$$_{2}\left(\widehat{\gamma}_{\text{(L-moment)}} \text{ and } \widehat{\tau}_{\text{(L-moment)}}\right) = \ell_2,$$

4.4. ADE

The ADE of $\widehat{\gamma}_{(ADE)}$ and $\widehat{\tau}_{(ADE)}$ are obtained by minimizing the function

$$\mathbf{ADE}(\gamma, \tau) = -n - n^{-1} \sum_{\hbar=1}^{n} (2\hbar - 1) \left\{ \log F_{(\gamma,\tau)}(z_{\hbar,n}) + \log\left[1 - F_{(\gamma,\tau)}(z_{-\hbar+1+n:n})\right] \right\}.$$

The parameter estimates of $\widehat{\gamma}_{(ADE)}$ and $\widehat{\tau}_{(ADE)}$ follow by solving the nonlinear equations

$$\frac{\partial}{\partial \gamma}\left[\mathbf{ADE}(\gamma, \tau)\right] = 0,$$

and

$$\frac{\partial}{\partial \tau}\left[\mathbf{ADE}(\gamma, \tau)\right] = 0.$$

4.5. RADE

The RTADE of $\widehat{\gamma}_{\text{(RADE)}}$ and $\widehat{\tau}_{\text{(RADE)}}$ are obtained by minimizing the function

$$\mathbf{RADE}(\gamma, \tau) = \frac{n}{2} - 2\sum_{\hbar=1}^{n} F_{(\gamma,\tau)}(z_{\hbar,n}) - \frac{1}{n} \sum_{\hbar=1}^{n} (2\hbar - 1) \left\{ \log\left[1 - F_{(\gamma,\tau)}(z_{-\hbar+1+n:n})\right] \right\}.$$

The parameter estimates of $\widehat{\gamma}_{\text{(RADE)}}$ and $\widehat{\tau}_{\text{(RADE)}}$ follow by solving the nonlinear equations

$$\frac{\partial}{\partial \gamma}\left[\mathbf{RADE}(\gamma, \tau)\right] = 0,$$

and

$$\frac{\partial}{\partial \tau}\left[\mathbf{RADE}(\gamma, \tau)\right] = 0.$$

4.6. LADE

The RTADE of $\widehat{\gamma}_{(\mathrm{LADE})}$ and $\widehat{\tau}_{(\mathrm{LADE})}$ are obtained by minimizing the function

$$\mathbf{LADE}\,(\gamma,\tau)=-\frac{3n}{2}+2\sum_{\hbar=1}^{n}F_{(\gamma,\tau)}(z_{\hbar,n})-\frac{1}{n}\sum_{\hbar=1}^{n}(2\hbar-1)\log F_{(\gamma,\tau)}(z_{\hbar,n}).$$

The parameter estimates of $\widehat{\gamma}_{(\mathrm{LADE})}$ and $\widehat{\tau}_{(\mathrm{LADE})}$ follow by solving the nonlinear equations

$$\frac{\partial}{\partial\gamma}\left[\mathbf{LADE}\,(\gamma,\tau)\right]=0,$$

and

$$\frac{\partial}{\partial\tau}\left[\mathbf{LADE}\,(\gamma,\tau)\right]=0.$$

Table 3: Simulation results for parameters $\tau=0.3$ and $\gamma=0.9$.

	n	BIAS$_{(\tau)}$	BIAS$_{(\gamma)}$	RMSE$_{(\tau)}$	RMSE$_{(\gamma)}$	D-abs	D-max
MLE	20	0.00473	−0.00128	0.02482	0.15916	0.00886	0.01439
CVME		0.01504	0.15410	0.06820	0.52117	0.03298	0.04917
L-moment		0.00470	−0.00174	0.02627	0.14546	0.00903	0.01456
ADE		0.00004	0.05892	0.05117	0.36210	0.02424	0.03377
RADE		0.00466	0.10184	0.05284	0.45873	0.03254	0.04543
LADE		0.01254	0.09170	0.06455	0.40016	0.01526	0.02490
MLE	60	0.00229	−0.00556	0.01352	0.09339	0.00643	0.00976
CVME		0.00577	0.04493	0.03447	0.20409	0.00849	0.01349
L-moment		0.00188	−0.00267	0.01418	0.08550	0.00447	0.00696
ADE		0.00082	0.01823	0.02773	0.16925	0.00624	0.00870
RADE		0.00265	0.03123	0.02778	0.18466	0.00837	0.01202
LADE		0.00103	0.01322	0.03474	0.18199	0.00377	0.00536
MLE	100	0.00128	−0.00202	0.01065	0.07658	0.00314	0.00486
CVME		0.00422	0.02960	0.02443	0.13867	0.00509	0.00838
L-MOMENT		0.00071	0.00085	0.01071	0.06603	0.00091	0.00165
ADE		0.00125	0.01512	0.02039	0.12088	0.00419	0.00599
RADE		0.00207	0.02178	0.02167	0.13518	0.00552	0.00803
LADE		0.00085	0.01225	0.02717	0.13770	0.00369	0.00521
MLE	200	0.00042	0.00021	0.00716	0.05173	0.00066	0.00113
CVME		0.00092	0.00845	0.01763	0.09965	0.00195	0.00292
L-moment		0.00025	0.00099	0.00753	0.04673	0.00014	0.00027
ADE		−0.00052	0.00157	0.01485	0.08804	0.00158	0.00238
RADE		−0.00027	0.00379	0.01523	0.09535	0.00209	0.00298
LADE		0.00171	0.01170	0.01981	0.100038	0.00201	0.00332

5. Simulation studies for comparing estimation methods

In this section, we perform a numerical simulation in order to compare the estimation methods. The simulation study is based on 1000 generated data sets from the LENH distribution for different sample sizes ($n=$

$20, 60, 100$ and 200) and different values of parameters as follows

	τ	γ
I	0.3	0.9
II	0.4	2.0
III	0.2	0.7

The estimates are compared in terms of their bias ($\text{BIAS}_{(\cdot)}$), the root mean-standard error ($\text{RMSE}_{(\cdot)}$), the mean of the absolute difference between the theoretical and the estimates (D-abs) and the maximum absolute difference between the true parameters and estimates (D-max) given by

$$\text{BIAS}_{(\cdot)} = \frac{1}{B}\sum_{\hbar=1}^{n}\left(\widehat{\cdot}_{\hbar} - \cdot\right), \ \text{RMSE}_{(\cdot)} = \sqrt{\frac{1}{B}\sum_{\hbar=1}^{n}\left(\widehat{\cdot}_{\hbar} - \cdot\right)^2},$$

$$\text{D-abs} = \frac{1}{nB}\sum_{\hbar=1}^{n}\sum_{j=1}^{n}\left|F_{(\gamma,\tau)}(z_{\hbar j}) - F_{(\widehat{\gamma},\widehat{\tau})}(t_{\hbar j})\right|$$

and

$$\text{D-abs} = \frac{1}{B}\sum_{\hbar=1}^{n}\max_{j}\left|F_{(\gamma,\tau)}(z_{\hbar j}) - F_{(\widehat{\gamma},\widehat{\tau})}(z_{\hbar j})\right|.$$

Table 4: Simulation results for parameters $\tau = 0.4$ and $\gamma = 2$

	n	$\text{BIAS}_{(\tau)}$	$\text{BIAS}_{(\gamma)}$	$\text{RMSE}_{(\tau)}$	$\text{RMSE}_{(\gamma)}$	D-abs	D-max
MLE	20	0.00402	−0.01721	0.02060	0.33785	0.01240	0.01885
CVME		0.01188	0.37288	0.05670	1.18611	0.03723	0.05330
L-moment		−0.00346	0.01299	0.01450	0.31305	0.01046	0.01590
ADE		−0.00135	0.12839	0.04475	0.83397	0.02694	0.03788
RTADE		0.00376	0.28602	0.04999	1.19537	0.04218	0.05866
LEADE		0.01097	0.36370	0.06462	1.13433	0.03808	0.05390
MLE	60	0.00166	−0.01130	0.01151	0.20354	0.00600	0.00893
CVME		0.00586	0.14362	0.03218	0.53921	0.01305	0.01932
L-moment		−0.00112	0.00364	0.00931	0.18177	0.00327	0.00501
ADE		0.00171	0.07361	0.02645	0.43795	0.00995	0.01384
RADE		0.00336	0.11205	0.02753	0.50223	0.01318	0.01856
LADE		0.00231	0.07360	0.03221	0.46851	0.00856	0.01211
MLE	100	0.00062	0.00079	0.00899	0.16224	0.00126	0.00205
CVME		0.00241	0.06383	0.02388	0.36720	0.00651	0.00944
L-moment		−0.00058	0.00233	0.00784	0.14181	0.00178	0.00272
ADE		−0.00016	0.02535	0.02030	0.31823	0.00520	0.00728
RADE		0.00050	0.04265	0.02155	0.36074	0.00696	0.00966
LADE		0.00187	0.05046	0.02486	0.36018	0.00526	0.00759
MLE	200	0.00031	−0.00013	0.00606	0.10972	0.00073	0.00116
CVME		0.00132	0.03926	0.01674	0.25589	0.00442	0.00630
L-moment		−0.00011	0.00106	0.00583	0.09760	0.00046	0.00068
ADE		0.00024	0.02174	0.01415	0.22299	0.00360	0.00500
RADE		0.00119	0.03294	0.01502	0.24789	0.00353	0.00506
LADE		0.00070	0.02157	0.01672	0.23368	0.00252	0.00357

Table 5: Simulation results for parameters $\tau = 0.2$ and $\gamma = 0.7$

	n	BIAS$_{(\tau)}$	BIAS$_{(\gamma)}$	RMSE$_{(\tau)}$	RMSE$_{(\gamma)}$	D-abs	D-max
MLE	20	0.00450	−0.00554	0.01957	0.122421	0.01277	0.02003L
CVME		0.01401	0.11141	0.05329	0.36718	0.02573	0.04115
L-moment		0.00504	−0.00842	0.02040	0.12373	0.01543	0.02396
ADE		0.00213	0.04348	0.03824	0.25034	0.01841	0.02570
RADE		0.00668	0.08084	0.03901	0.31553	0.02708	0.03883
LADE		0.00788	0.07403	0.05619	0.32343	0.02096	0.03166
MLE	60	0.00160	−0.00125	0.01122	0.07858	0.00416	0.00668
CVME		0.00541	0.03850	0.02628	0.15230	0.00890	0.01456
L-moment		0.00119	0.00007	0.01071	0.07131	0.00258	0.00432
ADE		0.00186	0.02082	0.02133	0.12920	0.00719	0.01039
RADE		0.00270	0.02981	0.02129	0.13834	0.01006	0.01462
LADE		0.00251	0.01978	0.02863	0.14331	0.00524	0.00822
MLE	100	0.00100	−0.00191	0.00800	0.05640	0.00322	0.00496
CVME		0.00335	0.01899	0.01997	0.10519	0.00361	0.00622
L-moment		0.00079	−0.00065	0.00804	0.05495	0.00207	0.00333
ADE		0.00101	0.00865	0.01632	0.09268	0.00252	0.00383
RADE		0.00115	0.01145	0.01658	0.10442	0.00371	0.00547
LADE		0.00248	0.01614	0.02052	0.10120	0.00335	0.00591
MLE	200	0.00031	0.00058	0.00565	0.04125	0.00037	0.00076
CVME		0.00163	0.01087	0.01346	0.07328	0.00246	0.00409
L-moment		0.00023	0.00092	0.00570	0.03955	0.00017	0.00029
ADE		0.00038	0.00503	0.01113	0.06503	0.00192	0.00273
RADE		0.00064	0.00769	0.01177	0.07143	0.00280	0.00401
LADE		0.00056	0.00426	0.01504	0.07301	0.00112	0.00177

From Tables 3, 4 and 5 we conclude that:

1-The biases tend to zero when n increases which means that all estimators are non-biased.

2-The RMSEs tend to zero when n increases which means incidence of consistency property.

6. Data analysis

6.1. Comparing estimation methods

An application to real data sets is introduced for comparing the estimation methods. We consider the Cramér-Von Mises (W*) and the Anderson-Darling (A*) statistics. The data consist of 72 exceedances for the years 1958–1984, rounded to one decimal place (Choulakian and Stephens (2001)): 1.7, 2.2, 14.4, 1.1, 0.4, 20.6, 5.3, 0.7, 1.9, 13.0, 12.0, 9.3, 1.4, 18.7, 8.5, 25.5, 11.6, 14.1, 22.1, 1.1, 2.5, 14.4, 1.7, 37.6, 0.6, 2.2, 39.0, 0.3, 15.0, 11.0, 7.3, 22.9, 1.7, 0.1, 1.1, 0.6, 9.0, 1.7, 7.0, 20.1, 0.4, 2.8, 14.1, 9.9, 10.4, 10.7, 30.0, 3.6, 5.6, 30.8, 13.3, 4.2, 25.5, 3.4, 11.9, 21.5, 27.6, 36.4, 2.7, 64.0, 1.5, 2.5, 27.4, 1.0, 27.1, 20.2, 16.8, 5.3, 9.7, 27.5, 2.5, 27.0. From Table 6 we conclude that the MLE method is the best method with W*=0.11682 and A*=0.66386 then L-moment with W*=0.11809 and A*=0.67000, however all other methods performed well. Figure 4 gives the Kaplan-Meier survival plots for

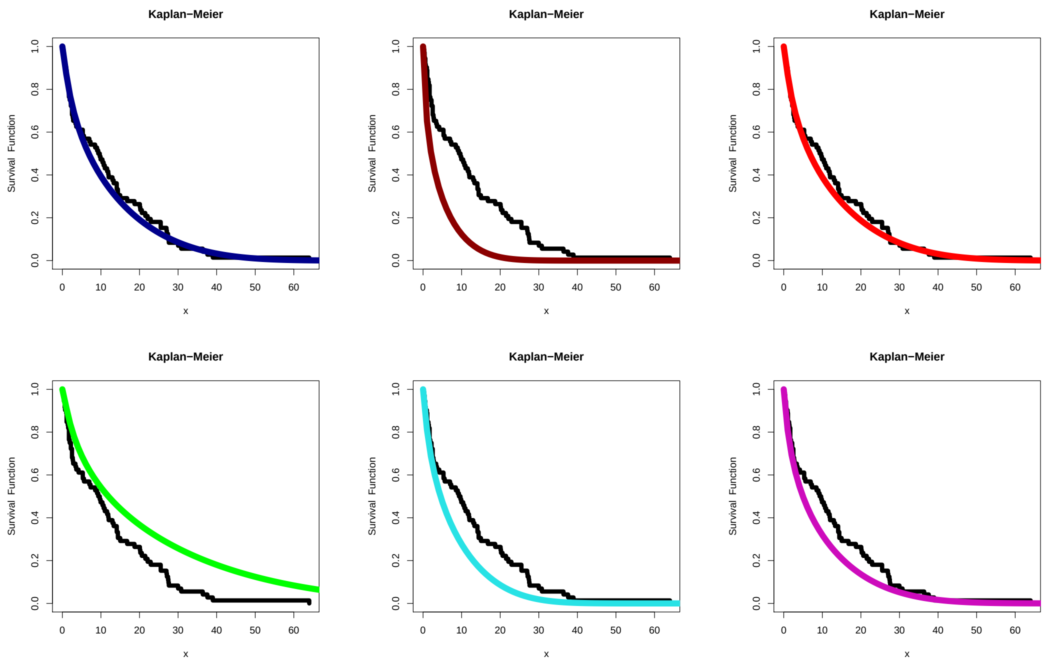

Figure 4. Kaplan-Meier survival plots for comparing methods.

comparing methods. Figure 5 gives the Probability-Probability (P-P) plots for comparing methods.

Table 6: The values of estimators, W* and A*.

Method	$\widehat{\tau}$	$\widehat{\gamma}$	W*	A*
MLE	0.268	1.047	**0.11682**	**0.66386**
CVM	0.237	0.879	0.13626	0.75904
L-moment	0.266	1.032	0.11809	0.67000
ADE	0.246	0.916	0.13026	0.72948
RADE	0.262	1.030	0.12058	0.68082
LADE	0.236	0.870	0.13714	0.76359

6.2. Comparing competitive models

We analyze an environmental real data set to show the LENH distribution flexibility. We compare LENH with some important NH versions. Some competitive models are listed in Table 7.

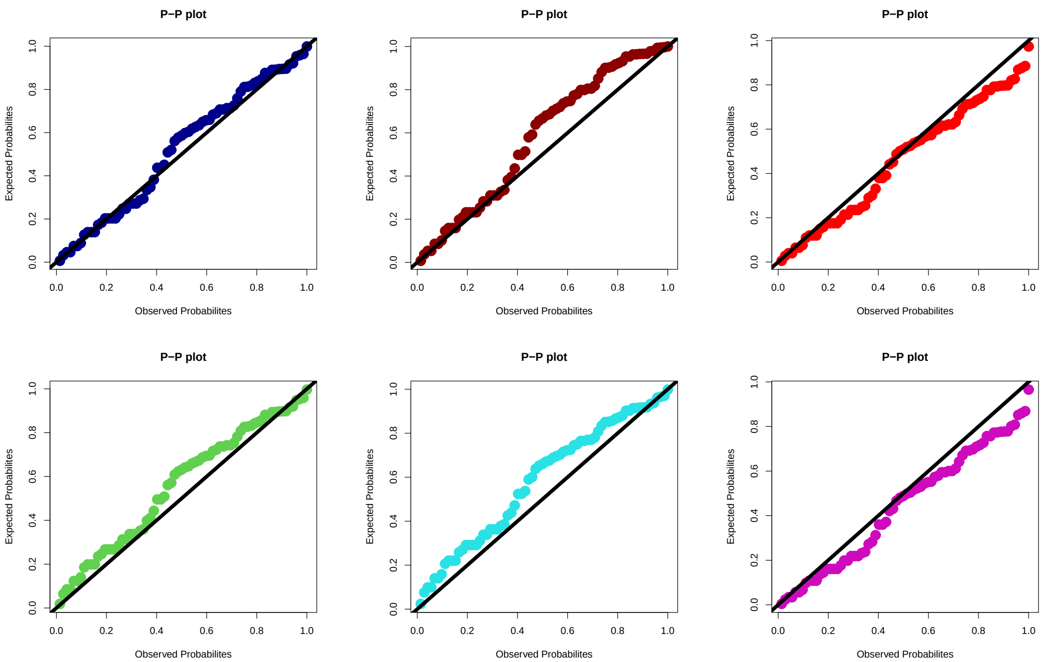

Figure 5. P-P plots for comparing methods.

Table 7: Some competitive models

N	Model	Abbreviation	Author
1	Gamma-NH	GaNH	Ortega et al. [32]
2	Marshall-Olkin-NH	MONH	Lemonte et al. [21]
3	Generalized-NH	GNH (ENH)	Lemonte [20]
4	Odd Lindley-NH	OLNH	Yousof et al. [42]
5	Proportional reversed hazard rate-NH	PRHRNH	-
6	odd log-logistic-NH	OLLNH	Ibrahim [19]
7	beta-NH	BNH	Dias et al. [12]
8	Nadarajah-Haghighi	NH	Nadarajah and Haghighi [30]
9	Rayleigh-NH	RNH	Elsayed and Yousof [15]

Figure 6 gives the skewness-kurtosis plot (or the Cullen and Frey plot) for exploring initial fit to the theoretical distributions such as normal, uniform, exponential, logistic, beta, lognormal and Weibull distributions. Cullen and Frey plot just compare distributions in the space of (squared skewness, kurtosis), this is a good summary but still only a summary of the properties of a distribution, heance many other many other graphical techniques are considered sush ad the “nonparametric Kernel density estimation” approach for exploring initial exceedances of flood peaks density shape, the “ Quantile-Quantile” plot for exploring “ normality” of the exceedances of flood peaks data, the “total time in test” plot for exploring the initial shape of the empirical HRF of the exceedances of flood peaks data, the “box plot” for exploring the extreme exceedances of flood peaks. For revealing the correlation between any two values of the signal changes as their separation changes,the autocorrelation function (ACF) is presented for the exceedances of flood peaks. The theoretical ACF is a time domain measure of the stochastic process memory, and does not reveal any information about the frequency content of the process. The theoretical ACF provides some information about the distribution of hills and valleys across the surface with Lag=1. The

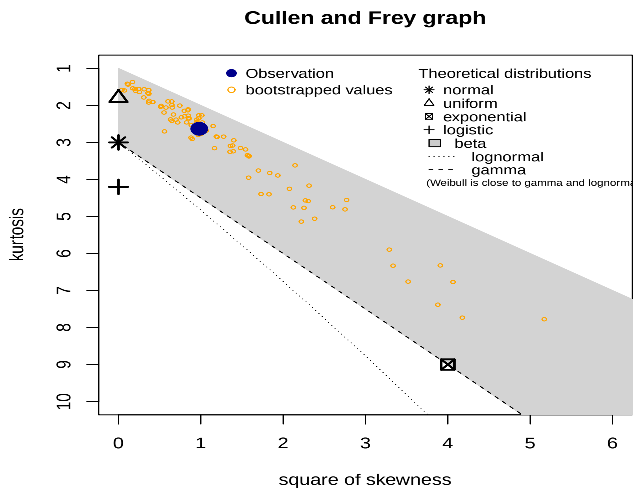

Figure 6. Cullen and Frey plot for exceedances of flood peaks data.

theoretical partial ACF with Lag= 1 is also presented. Figure 7 shows the scattergrams, ACF and partial ACF for exceedances of flood peaks data under Lag= 1.

In the applications, the information about the HRF can help in selecting a particular statistical model. For this aim, a device called the total time on test (TTT) plot (Aarset [1]) is useful. The TTT plot for the exceedances of flood peaks data (Choulakian and Stephens [11]) is given in Figure 8 (top left panel). Based on Figure 8 (top left panel), we conclude that the flood peaks data has a "bathtub" HRF (or **U**-HRF) which includes the "decreasing", "constant" and "increasing" HRF. Checking out Figure 8, we conculde that the our new model incudes the "decreasing", "constant" and "increasing" HRF. Figure 8 (top right panel) gives the box for exceedances of flood peaks data. Statisticians have developed a remarkably powerful set of tools for analyzing normally distributed data. The most popular one is the "normal quantile-quantile (Q-Q) plot". If the distribution of the data matched the normal distribution perfectly, all the quantile points would lie between the two blue lines. Figure 8 (bottom left panel) gives the Q-Q plot for exceedances of flood peaks data. Nonparametrically, for exploring the initial shape of real data the kernel density estimation is provided in Figure 8 (bottom right panel). Based on Figure 8 (bottom right panel), it is noted that the exceedances of flood peaks data is symmetric right skewed.

The model selection is applied using the estimated log-likelihood $\left(\widehat{\ell}\right)$, Akaike information criterion (C_1), Consistent Akaike Information Criteria (C_2), Bayesian information criterion (C_3), and Hannan-Quinn information criterion (C_4). All calculations are obtained by maxLik routine in R programme. Figure 9 give the estimated PDF (EPDF), estimated CDF (ECDF) and estimated HRF (EHRF) plots. Table 8 give the estimates of the competitive models along with its corresponding standard errors (SEs). Table 9 give statistics of the competitive models. The results displayed in Table 9 show that the LENH distribution has the lowest C_1, C_2, C_3 and C_4 and has the biggest estimated log-likelihood among all the fitted models. So it could be taken as the best one under these criteria among all the fitted models. Finally, we plot the estimated PDF, estimated CDF and estimated HRF of the LENH for the exceedances of flood peaks data in Figure 9. Clearly, the LENH distribution provides a closer fit to the empirical PDF and CDF. The P-P and Kaplan-Meier survival plots of the LENH for the exceedances of flood peaks data are given in Figure 10.

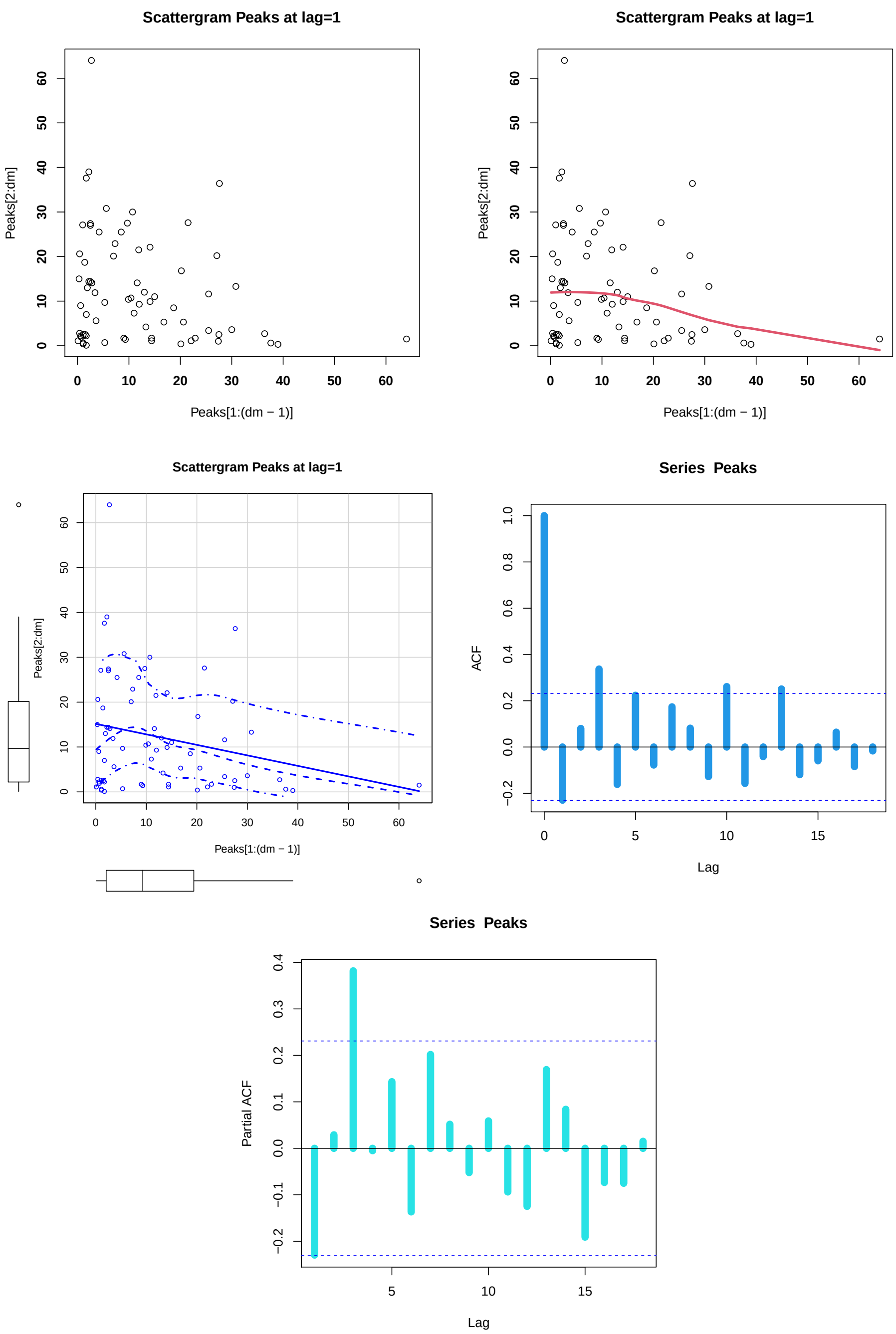

Figure 7. Scattergrams and autocorrelation function for peaks data.

7. Conclusions

A new two-parameter lifetime distribution called the odd Lindley exponentiated Nadarajah Haghighi (LENH) is proposed and numerically studied. The new model has a flexible failure rate shapes such as “monotonically

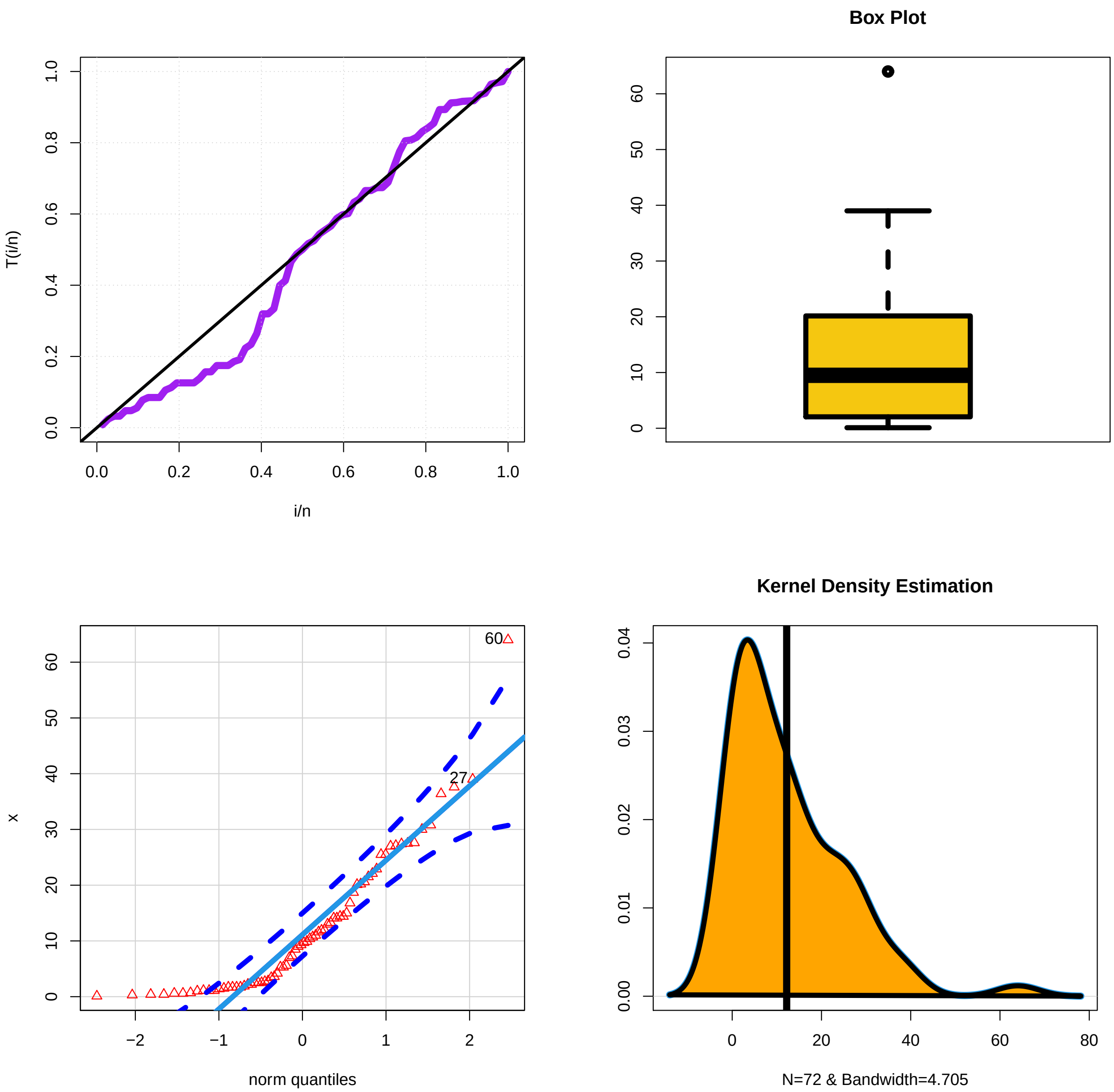

Figure 8. TTT, box, Q-Q and Kernel plots for the exceedances of flood peaks data.

increasing”, “monotonically decreasing”, “bathtub”, “constant”, “upside down” and “**J**-shape”. Various of its statistical properties are derived. A numerical analysis of skewness and kurtosis are presented and we noted that:

1- The skewness of the LENH model always positive.

2- The kurtosis of the LENH model can be more than three or less than three.

3- The expected value of the LENH model increases as γ increases.

4- The expected value of the LENH model decreases as τ increases.

5-The skewness of the LENH can range in the interval (0.4455, 33.07), whereas the skewness of the ENH varies only in the interval (0.51335, 3.5726). The spread for the LENH kurtosis is ranging from 2.8786 to 3749, whereas the spread for the ENH kurtosis only varies from 3.419 to 32.041. So it is clear that the new model is more flexible

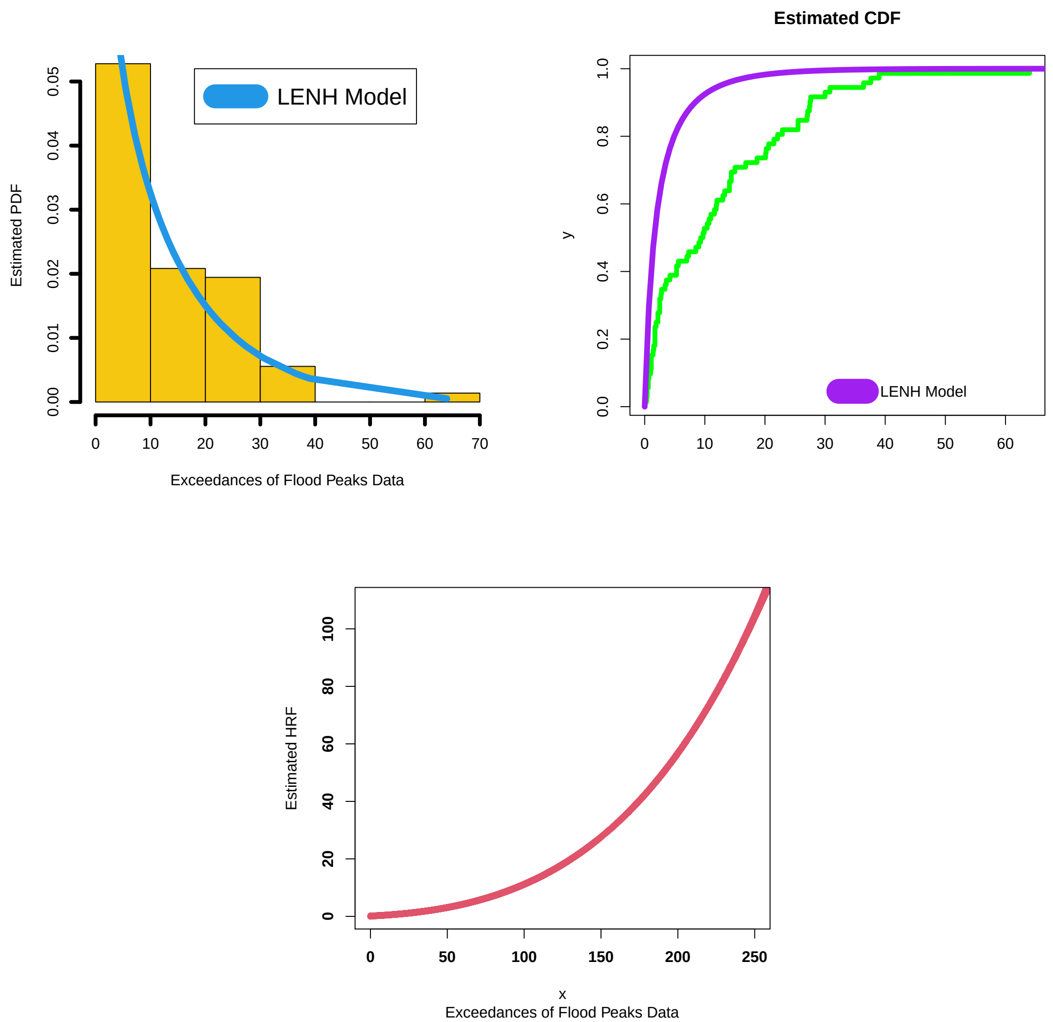

Figure 9. Estimated PDF, estimated CDF and estimated HRF plots for the exceedances of flood peaks data.

than the base line one. Many bivariate and multivariate extensions are also presented via Morgenstern family and Clayton Copula. Several estimation methods are such as the maximum likelihood, Cramér-von-Mises, L-moment estimation, Anderson Darling, right tail-Anderson Darling estimation, lest tail-Anderson Darling estimation are presented and considered. Numerical simulations are performed to assess the performance of estimation methods and we concluded that the biases tend to zero when n increases which means that all estimators are non-biased and the RMSEs tend to zero when n increases which means incidence of consistency property. Illustration of an environmental data set is employed to measure flexibility of the new model, the new model is the best one among all selected competitive models. Another application to compare the estimation methods is presented and we conclude that the MLE method is the best method with W^*=0.1168 and A^*=0.6639 then L-moment with W^*=0.1181 and A^*=0.670, however all other methods performed well. Following Altun [6], [7], [8], [9], Altun et al. [10] and Yousof [39], the LENH can be used for introducing a new log regression model for the censored real data modeling and future prediction.

Acknowledgement

The authors gratefully acknowledge with thanks the very thoughtful and constructive comments and suggestions of the Editor-in-Chief and the reviewers which resulted in much improved paper.

Table 8: Estimates of the competitive models fitted to the Choulakian and Stephens data.

Model	Estimates (SEs)			
LENH(γ, τ)	**1.04718**	**0.2679**		
	(0.1623)	**(0.0188)**		
Exp(b)	0.082			
	(0.01)			
NH(τ, b)	0.841	0.1094		
	(0.259)	(0.059)		
RNH(τ, b)	0.125	6.28		
	(0.012)	(2.919)		
OLLNH(γ, τ, b)	0.777	1.501	0.051	
	(0.105)	(0.685)	(0.033)	
OLNH(γ, τ, b)	0.7293	0.2519	1.8065	
	(0.6059)	(0.052)	(3.355)	
PRHRNH(γ, τ, b)	0.364	1.714	0.031	
	(0.068)	(1.191)	(0.031)	
GaNH(γ, τ, b)	0.7286	1.9299	0.0242	
	(0.1385)	(1.7591)	(0.0312)	
MONH(γ, τ, b)	23.77	0.0011	0.2660	
	(5.5053)	(0.0003)	(0.0895)	
GaNH(γ, τ, b)	0.7289	1.7126	0.0309	
	(0.1404)	(1.2607)	(0.0330)	
BNH(γ, a, τ, b)	0.8381	316.0285	0.6396	0.0003
	(0.1215)	(4.2194)	(0.8227)	(0.0004)
EWNH(γ, a, τ, b)	2.7591	0.3989	0.4732	0.6129
	(1.742)	(0.167)	(0.158)	(0.959)

Table 9: Statistics of the competitive models fitted to the Choulakian and Stephens data.

Model	Log-L	C_1	C_2	C_3	C_4
LENH	**−250.036**	**505.27**	**505.45**	**509.83**	**507.085**
OLLNH	−250.41	506.82	507.18	513.65	509.54
RNH	−251.722	507.44	507.62	513.99	509.7
NH	−251.987	507.97	508.15	515.53	509.79
OLNH	−250.589	507.18	507.53	514.01	509.9
PRHRNH	−300.83	607.66	608.02	614.49	610.38
GaNH	−250.917	507.834	508.187	514.66	510.55
MONH	−251.087	508.175	508.53	515.005	510.894
EWNH	−250.032	508.064	508.66	517.17	511.69
ENH	−250.925	507.849	508.202	514.679	510.57
BNH	−251.356	510.713	511.31	519.82	514.34
Exp	−252.128	506.256	506.313	513.533	507.162

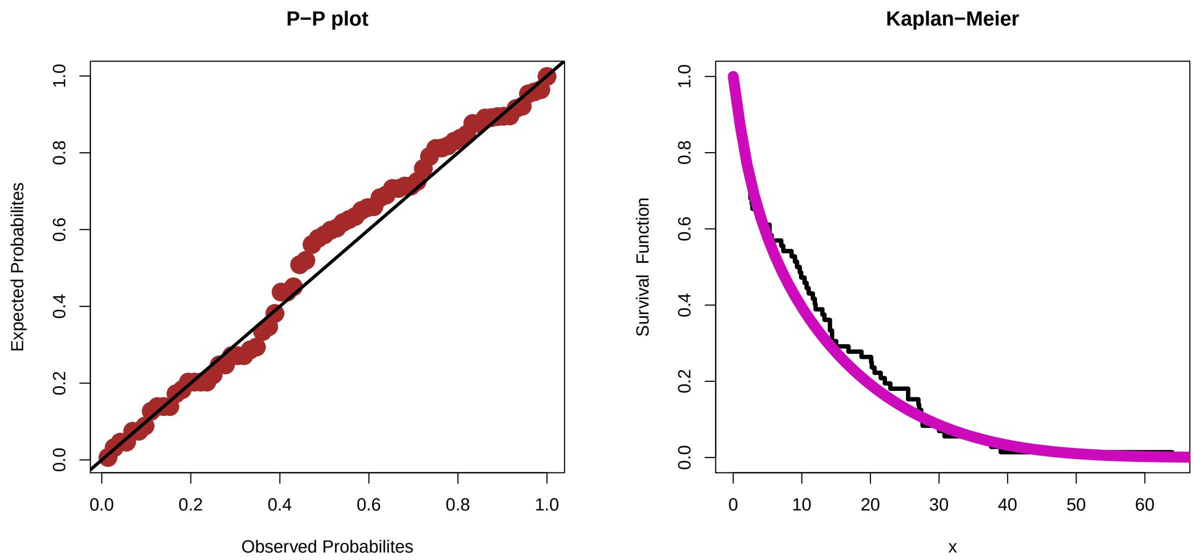

Figure 10. P-P and Kaplan-Meier survival plots for the exceedances of flood peaks data.

REFERENCES

1. Aarset, M. V. *How to identify bathtub hazard rate*. IEEE Transactions on Reliability, 36, pp. 106-108, 1987.
2. Ali, M. M., Yousof, H. M. and Ibrahim, M. *A new version of the generalized Rayleigh distribution with copula, properties, applications and different methods of estimation*. Optimal Decision Making in Operations Research & Statistics: Methodologies and Applications, VOL 1, pp. 1-25, 2021a.
3. Ali, M. M., Ibrahim, M. and Yousof, H. M. *Expanding the Burr X model: properties, copula, real data modeling and different methods of estimation*. Optimal Decision Making in Operations Research & Statistics: Methodologies and Applications, VOL 1, pp. 26-49, 2021b.
4. Al-babtain, A. A., Elbatal, I. and Yousof, H. M. *A new flexible three-parameter model: properties, Clayton copula, and modeling real data*. Symmetry, 12(3), pp. 440, 2020.
5. Alizadeh, M., Rasekhi, M., Yousof, H. M., Ramires, T. G. and Hamedani G. G. *Extended exponentiated Nadarajah-Haghighi model: mathematical properties, characterizations and applications*. Studia Scientiarum Mathematicarum Hungarica, 55, pp. 498–522, 2018.
6. Altun, E., Yousof, H. M. and Hamedani G. G. *A new flexible extension of the generalized half-normal lifetime model with characterizations and regression modeling*. Bulletin of Computational Applied Mathematics, 6(1), pp. 83-115, 2018a.
7. Altun, E., Yousof, H. M. and Hamedani, G. G. *A new generalization of generalized half-normal distribution: properties and regression models*. Journal of Statistical Distributions and Applications, 5(1), pp. 7, 2018b.
8. Altun, E., Yousof, H. M. and Hamedani, G. G. *A new log-location regression model with influence diagnostics and residual analysis*. Facta Universitatis, Series: Mathematics and Informatics, 33(3), pp. 417-449, 2018c.
9. Altun, E., Yousof, H. M. and Hamedani G. G. *A Flexible Extension of Generalized Half-Normal Distribution: Characterizations and Regression Models*. International Journal of Applied Mathematics and Statistics, 57(3), pp. 27-49, 2018d.
10. Altun, E., Yousof, H. M., Chakraborty, S. and Handique, L. *Zografos-Balakrishnan Burr XII distribution: regression modeling and applications*. International Journal of Mathematics and Statistics, 19(3), pp. 46-70, 2018.
11. Choulakian, V., Stephens, M.A. *Goodness-of-fit for the generalized Pareto distribution*. Technometrics, 43, pp. 478–484, 2001.
12. Dias, C. R. B., Alizadeh, M. and Cordeiro, G. M. The beta Nadarajah-Haghighi distribution. Hacettepe Journal of Mathematics and Statistics, 47, pp. 1302-1323, 2018.
13. Elgohari, H. and Yousof, H. M. *A Generalization of Lomax Distribution with Properties, Copula and Real Data Applications*. Pakistan Journal of Statistics and Operation Research, 16(4), pp. 697-711, 2020a. https://doi.org/10.18187/pjsor.v16i4.3260
14. Elgohari, H. and Yousof, H. M. *New Extension of Weibull Distribution: Copula, Mathematical Properties and Data Modeling*. Statistics, Optimization & Information Computing, 8(4), pp. 972-993, 2020b. https://doi.org/10.19139/soic-2310-5070-1036
15. Elsayed, H. A. H. and Yousof, H. M. *The Burr X Nadarajah Haghighi distribution: statistical properties and application to the exceedances of flood peaks data*. Journal of Mathematics and Statistics, 15, pp. 146-157, 2019.
16. Gupta, R.D. and Kundu, D. *Generalized exponential distributions*. Aust. N. Z. J. Stat. 41, pp. 173–188, 1999.
17. Gumbel, E. J. *Bivariate logistic distributions*. Journal of the American Statistical Association, 56, pp. 335-349, 1961.
18. Gumbel, E. J. *Bivariate exponential distributions*. Journal of the American Statistical Association, 55, pp. 698-707, 1960.

19. Ibrahim, M. *The generalized odd log-logistic Nadarajah Haghighi distribution: statistical properties and different methods of estimation*. J. Appl. Probab. Stat, 15, pp. 61-84, 2020.
20. Lemonte, A. J. *A new exponential-type distribution with constant, decreasing, increasing, upside-down bathtub and bathtub-shaped failure rate function*. Computational Statistics & Data Analysis, 62, 149-170, 2013.
21. Lemonte, A. J., Cordeiro, G. M. and Moreno–Arenas, G. *A new useful three-parameter extension of the exponential distribution*. Statistics, 50(2), pp. 312-337, 2016.
22. MacDonald, P. D. M. *Comment on An estimation procedure for mixtures of distributions by Choi and Bulgren*. Journal of the Royal Statistical Society. Series B, 33(2), pp. 326-329, 1971.
23. Mansour, M. M., Ibrahim, M., Aidi, K., Shafique Butt, N., Ali, M. M., Yousof, H. M. and Hamed, M. S. *A New Log-Logistic Lifetime Model with Mathematical Properties, Copula, Modified Goodness-of-Fit Test for Validation and Real Data Modeling*. Mathematics, 8(9), pp. 1508, 2020a.
24. Mansour, M. M., Butt, N. S., Ansari, S. I., Yousof, H. M., Ali, M. M. and Ibrahim, M. *A new exponentiated Weibull distribution's extension: copula, mathematical properties and applications*. Contributions to Mathematics, 1 (2020), pp. 57–66, 2020b. DOI: 10.47443/cm.2020.0018
25. Mansour, M., Korkmaz, M. C., Ali, M. M., Yousof, H. M., Ansari, S. I. and Ibrahim, M. *A generalization of the exponentiated Weibull model with properties, Copula and application*. Eurasian Bulletin of Mathematics, 3(2), pp. 84-102, 2020c.
26. Mansour, M., Rasekhi, M., Ibrahim, M., Aidi, K., Yousof, H. M. and Elrazik, E. A. *A New Parametric Life Distribution with Modified Bagdonavičius–Nikulin Goodness-of-Fit Test for Censored Validation, Properties, Applications, and Different Estimation Methods*. Entropy, 22(5), pp. 592, 2020d.
27. Mansour, M., Yousof, H. M., Shehata, W. A. and Ibrahim, M. *A new two parameter Burr XII distribution: properties, copula, different estimation methods and modeling acute bone cancer data*. Journal of Nonlinear Science and Applications, 13(5), pp. 223-238, 2020e.
28. Mansour, M. M., Butt, N. S., Yousof, H. M., Ansari, S. I. and Ibrahim, M. *A Generalization of Reciprocal Exponential Model: Clayton Copula, Statistical Properties and Modeling Skewed and Symmetric Real Data Sets*. Pakistan Journal of Statistics and Operation Research, 16(2), pp. 373-386, 2020f.
29. Morgenstern, D. *Einfache beispiele zweidimensionaler verteilungen*. Mitteilingsblattfur Mathematische Statistik, 8, pp. 234-235, 1956.
30. Nadarajah, S.and Haghighi, F. *An extension of the exponential distribution*. Statistics. 45, pp. 543–558, 2011.
31. Nascimento, A. D., Silva, K. F., Cordeiro, G. M., Alizadeh, M., Yousof, H. M. and Hamedani, G. G. *The odd Nadarajah-Haghighi family of distributions: properties and applications*. Studia Scientiarum Mathematicarum Hungarica, 56(2), pp. 185-210, 2019.
32. Ortega, E. M., Lemonte, A. J., Silva, G. O. and Cordeiro, G. M. *New flexible models generated by gamma random variables for lifetime modeling. Journal of Applied Statistics*, 42(10), pp. 2159-2179, 2015.
33. Pougaza, D. B. and Djafari, M. A. *Maximum entropies copulas*. Proceedings of the 30th international workshop on Bayesian inference and maximum. Entropy methods in Science and Engineering, pp. 329-336, 2011.
34. Rodriguez-Lallena, J. A. and Ubeda-Flores, M. *A new class of bivariate copulas*. Statistics and Probability Letters, 66, pp. 315-25, 2004.
35. Renyi, A. *On measures of entropy and information*. In: Proceedings of the Fourth Berkeley Symposium on Mathematical Statistics and Probability I, University of California Press, Berkeley, pp. 547-561, 1961.
36. Shannon, C.E. *A mathematical theory of communication*. Bell System Technical Journal. 27, 379-432, 1948.
37. Silva, F. S., Percontini, A., E., Ramos, de Brito, M. W., Venancio, R. and Cordeiro, G. M. *The Odd Lindley-G Family of Distributions*. Austrian Journal of Statistics, 46(1), pp. 65-87, 2017.
38. Yousof, H. M., Ali, M. M., Aidi, K., Hamedani, G. G. and Ibrahim, M. *A new lifetime distribution with properties, characterizations, validation testing, different estimation methods*. Statistics, Optimization & Information Computing, forthcoming 2021.
39. Yousof, H. M., Altun, E., Rasekhi, M., Alizadeh, M., Hamedani, G. G. and Ali, M. M. *A new lifetime model with regression models, characterizations and applications*. Communications in Statistics-Simulation and Computation, 48(1), pp. 264-286, 2019.
40. Yousof, H. M. and Korkmaz, M. C. *Topp-Leone Nadarajah-Haghighi distribution: mathematical properties and applications, International Journal of Applied Mathematics*. Journal of Statisticians: Statistics and Actuarial Sciences, 2, pp. 119-128, 2017.
41. Yousof, H. M., Hamedani, G. G. and Ibrahim, M. (2020). *The Two-parameter Xgamma Fréchet Distribution: Characterizations, Copulas, Mathematical Properties and Different Classical Estimation Methods*. Contributions to Mathematics, 2, 32-41, 2020.
42. Yousof, H. M., Korkmaz, M. C. Hamedani G. G. *The odd Lindley Nadarajah-Haghighi distribution*. J. Math. Comput. Sci., **7**, pp. 864-882, 2017.